NOAO AURA NSF

Teacher Leaders in Research Based Science Education

The RBSE Journal 2005

The RBSE Journal is an annual publication that presents the research of students and teachers who have participated in the Teacher Enhancement program TLRBSE, "Teacher Leaders in Research Based Science" at the National Optical Astronomy Observatory in Tucson. This program, funded by the NSF, consists of a distance learning course and a summer workshop for high school teachers interested in incorporating research and leadership mentoring within their class and school. TLRBSE brings the research experience to the classroom with datasets, materials, support and mentors during the academic year.

These papers represent a select set of those submitted for publication by many students. All papers are reviewed both by the Senior Editor and the Astronomer responsible for the particular research project. In addition to papers representing classroom work, a number of these papers are based on observing done at part of the Teacher Observing Program (TOP) at Kitt Peak during the fall and winter. More information about both the TLRBSE and the TOP program can be found on the website, www.noao.edu/outreach/tlrbse

I want to thank Dr. Travis Rector, Dr. Connie Walker, Dr. Steve Howell, and Dr. Jeff Lockwood for their generous help in reviewing these papers and working with the young scientists. Special thanks are due to Kathie Coil for her editing of the final copy.

Dr. Katy Garmany
Senior Editor, RBSE Journal

Table of Contents

SOLAR RESEARCH

The Association of Solar Magnetic Field Strength Variation with Sunspot Area 5
Leah J. Corpuz, Nick Gannon, and Damon Williams
Lincoln High School, Stockton, CA
Teacher: Babs Sepulveda, TLRBSE 2002

Sunspot Activity and Amount of Snowfall in Portland, Maine 11
Spencer Hudson
Biddeford Middle School, Biddeford, ME
Teacher: Barbara A. Fortier, TLRBSE 2004

The Effect of Sunspot Size and Latitude on Magnetic Field Strength in Sunspots .. 16
(TOP Research)
Sarah Mullins and Sheena Stanley
Linwood Holton Governor's School
Dr. Steve A. Rapp, TLRBSE 2002

NOVA RESEARCH

Magnitude and Lifespan of Centered Galactic Novae vs. Outer Edge Galactic Novae 26
Eric Kalver and Anthony Petrocchi
Cranston High School East, Cranston, RI
Teacher: Howard Chun, RBSE 1999

The Distance to M31 via a Cepheid 33
Barry G. Parker Jr.
Deer Valley High School, Antioch, CA
Teacher: Jeff Adkins, TLRBSE 2002

Nova Rate in M31 Galaxy 41
Liz Herndon and Sarah Green
Graves County High School, Mayfield, KY
Teacher: Velvet Dowdy, TLRBSE 2000

AGN RESEARCH

Redshifts of Starburst and Elliptical/Radio Galaxies 45
Joseph Dublin, Mark Ashley, Josh Keeling
Graves County High School, Mayfield, KY
Teacher: Velvet Dowdy, TLRBSE 2003

Measuring the Microvariability of BL Lac 50
(TOP Research)
Tri Nguyen
Deer Valley High School, Antioch, CA
Teacher: Jeff Adkins, TLRBSE 2002

VARIABLE STAR RESEARCH

RV Tauri Stars: Spectral Rebels 60
Nathan J. Stano, Graham T. Kozak, and Zackery J. Schroeder
Grosse Pointe North High School, Grosse Pointe Woods, MI
Teacher: Ardis Maciolek, RBSE 1998, TLRBSE 2001

Multiple Periodicities of RV- Tauri Variable Stars 67
(TOP Research)
Glenn Ferreira
Westford Academy, Westford, MA
Teacher: Joan Kadaras, TLRBSE 2003

Determining the Stellar Qualities of Stars Within Eclipsing Binary Systems 73
(TOP Research)
Kimmerlee Johnson
Great Falls High School, Great Falls MT
Teacher: Beth Thomas, TLRBSE 2000

A Study of Host Stars in Comparison with Stars without Planets, Using Spectrographs.. 82
(TOP Research)
Michelle Smith
Great Falls High School, Great Falls, MT
Teacher: Beth Thomas, TLRBSE 2004

The Association of Solar Magnetic Field Strength Variation with Sunspot Area

Leah J. Corpuz, Nick Gannon, and Damon Williams
Lincoln High School, Stockton, CA
Teacher: Babs Sepulveda, TLRBSE 2002

ABSTRACT

In this paper we address whether variation in solar magnetic field strength is related to sunspot area. We measure the area of selected sunspots on given days and then compare those measurements with the observed solar magnetic field strength on those same days. After collecting a sample size of ten pieces of data, graphing them, and running a linear regression T-test on the results, we conclude that there is an association between the sun's magnetic field strength and the area of sunspots.

INTRODUCTION

Sunspots are dark regions on the sun's surface (a.k.a. the photosphere) that are usually about 1800 K cooler than their surroundings[9]. A typical diameter for a large sunspot is around 32,000 km, though small sunspots – called pores – may have a diameter of only a few hundred km. Pores also lack the lighter area, called the penumbra, which surrounds larger sunspots. The dark spot itself is called the umbra[6]. These spots speckle the photosphere more or less constantly, the larger ones lasting for months, and the smaller ones for only a few hours. Where the sunspots occur and how many exist is dictated by an eleven-year sunspot cycle[5]. At the cycle's start, most sunspots are located between 20° and 40° south and north of the sun's equator. From there the sunspots multiply and creep closer to the equator until – at the height of the cycle – they've reached their greatest number and have come within 5° of the equator. After that zenith the sunspots begin to die off, particularly the ones further than 15° from the equator. The cycle ends with a minimum of sunspots before starting over again[1].

These odd blots on the sun's surface are interesting in their own right (which, really, would be enough of a reason to study them), but a particular topic of interest has been the alleged association between the number of sunspots and the Earth's climate. It has been often noted that the Little Ice Age of the mid-17th to early 18th centuries was concurrent with an unusually low amount of solar activity, sunspots included. This period of time is known as the Maunder Minimum[2]. One recent study in Science has shown there to be a possible link between solar activity and the climate of the North Atlantic[3].

So considering sunspots appear to influence Earth's climate, it's surprising we know so little about how they are created. Some astronomers think sunspots are created by hydromagnetic wave radiation that carries away thermal energy[8]. Some others think they're started by giant rings of turbulent, magnetic gas that lie beneath the photosphere and rotate perpendicular to the sun's equator. Wherever these rings bump together (the theory goes), a sunspot is created[6]. But the standard theory suggests that sunspots are created by changes in the solar magnetic field.

The sun's magnetic field is created by flows of plasma in the sun's convection zone, itself created by heat from the sun's fusion9. Since the sun rotates faster at its equator than at its poles, its strong magnetic fields are stretched out from east to west as the sun turns. This stretching out inhibits convection, allowing a spot on the sun to cool – and thus, a sunspot is born4. There have been other coincidences that seem to show a relationship between sunspots and the solar magnetic field, such as the fact that it (the field) changes poles simultaneously with the eleven-year sunspot cycle7. Yet the exact relationship between sunspots and the solar magnetic field remains unclear.

The purpose of our study is to see whether solar magnetic field strength does indeed vary with the area of sunspots, as the standard theory says it should.

OBSERVATION AND DATA REDUCTION

Daily observations of the sun are made with the Kitt Peak Vacuum Telescope, located in Arizona. Images of the sun are produced at three wavelengths by establishing a CCD camera at the spectrograph's focal plane. These images show the photosphere's brightness at a wavelength that roughly estimates the visual intensity of the photosphere in the "red" spectrum. The KPVT images have been processed to remove darkening and streaks.

Our physics instructor, Mrs. Sepulveda, gave us project software with these images stored in it. Using this software and the KPVT observations, we selected certain sunspots, measured their area, and then compared those measurements with the solar magnetic field strength on the corresponding date. (The measurements of solar magnetic field strength were provided by the National Optical Astronomy Observatories and were also collected on the software given us.)

After we collected the data, its analysis was carried out with the help of a Texas Instrument TI-83 calculator borrowed from the Lincoln High School library. This calculator specializes in statistical analyses. Its programmed tests were extremely useful in analyzing the data.

Data Table

Image Number	Sunspot Area (in sq. km)	Latitude of Sunspot	Longitude of Sunspot	Magnetic Area (in sq. km)
801	**5.12×10^8**	**16°**	**-17.3°**	**7.72×10^8**
802	**4.86×10^8**	**16.7°**	**-3.2°**	**6.13×10^8**
803	**4.35×10^8**	**17°**	**8.3°**	**6.73×10^8**
804	**3.94×10^8**	**16.9°**	**21.3°**	**9.46×10^8**
805	**4.31×10^8**	**17°**	**34.5°**	**7.51×10^8**
808	**7.1×10^8**	**18.3°**	**16.2°**	**1.31×10^9**
809	**7.05×10^8**	**18.3°**	**-3.3°**	**1.29×10^9**
810	**7.57×10^8**	**19.3°**	**9.8°**	**1.57×10^9**
812	**6.93×10^8**	**18.4°**	**37.4°**	**1.45×10^9**
821	**4.84×10^8**	**-10.3°**	**-10.1°**	**2.34×10^9**

ANALYSIS AND RESULTS

Figure 1

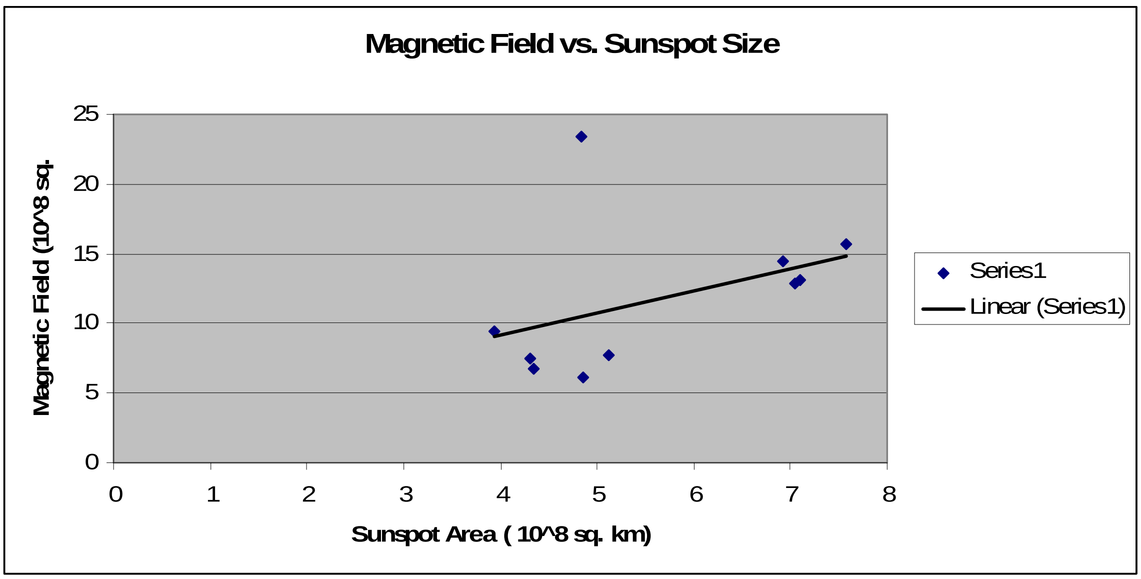

Our graphs showed that we have a normal set of data points as well as showing that there is a strong relation to the size (area) of a sunspot and the size of its surrounding magnetic field.

DISCUSSION

The scatterplot in Figure 1 seems to show a relationship between the size of a sunspot's area and its surrounding magnetic field strength. However, we cannot reach a conclusion on looks alone. The association we see might be imaginary or even due to chance. Therefore we have to carry out a test statistic to see whether or not there is a significant correlation between the two sets of data. The specific test we'll carry out is called a linear regression T-test. This requires us to first find the least squares regression line of the data, see how well this theoretical line fits reality, and then determine its p-value. (Of course, a low p-value means the probability that the variation in this data is due to chance is low.)

Even though a test is necessary to reach any conclusion at all, we must still proceed with caution. Ten pieces of data is not a very large sample size. In fact, it is conspicuously lower than the recommended thirty for this type of test. The sample size is also not random. Most of the sunspots we observed were located between 16° and 19° above the equator, and were selected because of the ease with which they could be measured. This could bias our results. Finally, the last sunspot we measured (labeled "Image Number 821") is an apparent outlier in our scatterplot. This is particularly worrisome because it is the only sunspot we measured that was located below the sun's equator. After some trepidation, we decided to remove this particular piece of data from the following analysis. Its presence is too influential and could confound our results.

Now we are ready to proceed with the test. Our null and alternate hypotheses are as follows:

H_o: There is no association between sunspot area and solar magnetic field strength.
H_a: There is an association between sunspot area and solar magnetic field strength.

This kind of hypothesis necessitates a two-tailed test, as we plan to do. We also plan to have an α-level of .05, as is standard for nonmedical scientific tests.

The data has to be normal for a linear regression t-test to work, so we first checked our data for normalcy by using a normal probability distribution (NPD) on both data sets. We were able to find the z-scores for all the pieces of data using the equation

$$(x - \mu)/\sigma = z$$

Incidentally, we did not find the mean or standard deviation by hand, but instead simply ran both data sets through a one-variable statistics test in our calculator. The NPD's show a straight diagonal plot for both sunspot and magnetic area, respectively, so we can confidently say that the data is normal.

After inserting the data into lists (with sunspot area as L_1 and magnetic area as L_2 – both designations being arbitrary), we ran them through the calculator's "LinReg(a+bx)" option under STAT:CALC. As the calculator's name for it already shows, this follows the equation y = a+bx. The least squares regression line for our data is

$$y = -2.504762229 + 2.270014836x.$$

After finding that, we were able to calculate the residuals for our data by subtracting the predicted value (as calculated from the equation above) from the magnetic field strength we actually observed. The residual plot is fairly scattered, so it seems this least squares regression line is a good fit for our data.

That done, we now had to find the correlation (a.k.a. "r") for our data. We accomplished this by 1) finding the z-score for all our pieces of data (as we already accomplished when we created out NPD's), 2) multiplying each two together, 3) adding the products, and 4) dividing by n-1, which in this case was 8. All this revealed a r^2-value of .80690956 and a r-value of .89828145. Such a high r-value means there is a strong association between sunspot area and solar magnetic field strength.

That answers our research question, but there is still a possibility that the correlation is due to chance. We therefore had to determine our data's p-value. This was easily accomplished by using the calculator's LinRegTTest (option E under STAT:TEST), with x still being sunspot area and y being magnetic area. We found the degrees of freedom for our data is seven (corresponding with the equation df = n-2), the t-value is 5.408552608, and the p-value is .00099928248.

This p-value is lower than our predetermined α-level of .05, so we can reject our null hypothesis and state that there is an association between sunspot area and solar magnetic field strength.

We did not encounter many difficulties in researching this project. Finding information on sunspots was easy. It is a frequently mentioned subject in astronomy books and Internet pages. Even finding relevant research articles was not too hard – it only required a judicious amount of flipping through back issues of science journals. With the help of the NIH imaging program provided to us, the gathering of precise data was not more that a mouse-click away. Although slightly repetitious at times, collecting the data was very straight forewarned. Testing our data for significance was not so much difficult as time-consuming, but the process – long as it was – never lapsed into tedium.

SUMMARY

Although our study reveals an association between sunspot area and variation in solar magnetic field strength, an association – even a very strong one – is not enough to prove causation. The apparent association may be due to a lurking variable (the bane of all scientists) that we cannot detect. Such a variable could falsely suggest a relationship between sunspot area and magnetic field strength while hiding the real relationship. Even if there is a relationship, it may be that sunspots are caused by more than simply variations in the solar magnetic field.

It is impossible to prove causation without an experiment. Nor have any of the other theories on sunspot creation been proven wrong. Sunspot creation, growth, and decay may still have a stronger relation to thermal waves, sub-photospheric gases, or any other variety of solar activities than they do the solar magnetic field. Even so, an association between sunspots and magnetic field strength has been strongly established by this and other studies, and further theorizing will probably take this into account.

Exactly how sunspots are formed – and how or whether this is related to the solar magnetic field – is still a mystery. The exact process of sunspot creation is still open to new theories.

REFERENCES

Athay, R. Grant. "Sun." *Encyclopedia Americana*. International Edition. 1991

Beckman, John E., and Terence J. Mahoney. "The Maunder Minimum and Climate Change: Have Historical Records Aided Current Research?" *Instituto de Astrofísica de Canarias.* 1998. Astronomical Society of the Pacific. 5 Mar. 2005 <http://www.stsci.edu/stsci/meetings/lisa3/beckmanj.html>

Bond et al., "Persistent Solar Influence on North Atlantic Climate During the Holocene," *Science* 2001 294: 2130-2136

Chapman, Gary. "On the energy balance of solar active regions." *Nature* 15 March 1984: 252-254

Hoskin, Michael, ed. *The Cambridge Illustrated History of Astronomy.* Cambridge, UK: Cambridge University Press, 1997

Pasachoff, Jay M. "Sunspot." *World Book Online Reference Center*. 2005. World Book, Inc. 4 Mar. 2005 <http://www.aolsvc.worldbook.aol.com/wb/Article?id=ar540040>.

Phillips, Tony. "The Sun Does a Flip."*Science @ NASA.* 15 Feb. 2001. Marshall Space Flight Center: Science and Technology Directorate. 4 Mar. 2005 <http://science.nasa.gov/headlines/y2001/ast15feb_1.htm>

Rast, M. P., P. A. Fox, H. Lin, B. W. Lites, R. W. Meisner, and O. R. White. "Bright rings around sunspots." *Nature* 14 Oct 1999: 678-679

Regents of the University of California. "Modern Research: The Sun's Magnetism." *Welcome to Sunspots.* 2001. UC Berkeley Center for Science Education at Space Sciences Laboratory. 4 Mar. 2005 <http://cse.ssl.berkeley.edu/segwayed/lessons/sunspots/research3.html>

Sunspot Activity and Amount of Snowfall in Portland, Maine

Spencer Hudson
Biddeford Middle School, Biddeford, ME
Teacher: Barbara A. Fortier, TLRBSE 2004

ABSTRACT

A relationship between the amount of snowfall in Portland, Maine and the seasonal average of sunspot numbers was analyzed. Examination of the snowfall record over the past 124 years revealed that Portland, Maine had fourteen winter seasons where it received over 100 inches of snow. Analysis of sunspot records for those same fourteen seasons showed a fluctuation in average sunspot numbers. It was therefore determined that a relationship between sunspot number and snowfall amount could not be substantiated for the Portland, Maine region.

INTRODUCTION

A relationship was examined between the monthly average sunspot number from October through May and snowfall amounts in Portland, Maine for these same months. Of the past 124 years, 14 seasons in Portland have seen more than 100 inches of snow. This study focuses on the relationship between sunspot number and snowfall amounts for those 14 seasons while comparing the data to the average sunspot number from October through May for the other 109 years.

The relationship between sunspot activity and snowfall amount has been studied before by scientists who believe there is a relationship between sunspot number and the amount of snowfall received in a given region. Scientists T. E. Osterkamp and T. Zhang did a study in Alaska in 1993 and found a snowfall periodicity cycle near 10 years. They reported that their findings showed this cycle closely followed the 11 year sunspot cycle.

William Deedler, a weather historian for the National Weather Service in Detroit/Pontiac, MI, also published a report in October 2004 in which he stated that sunspot activity would continue to wane and would bottom out in the next few years (with solar minimum expected around 2006). In his publication, he also noted a relationship between some of the more severe winters in Michigan and a lull in solar activity.

To obtain some background knowledge, sunspots were studied and found to be dark patches that are visible in the sun's photosphere. Sunspots appear darker than the surrounding material on the sun due to their cooler temperatures. These cooler temperatures can be attributed to a magnetic field that is approximately 1000 times stronger than the average magnetic field on the sun. One theory is that this strong, localized magnetic field inhibits gas motion blow the photosphere and reduces the convection of heat from rising gas within the sun to the sun's surface. Although they appear dark on the surface of the sun, their luminosity is actually brighter than a full moon!

Some sunspots can be as big as 50,000 miles in diameter - almost twice the circumference of earth! Sunspots can also fluctuate in shape and size, and they rotate along with the sun. Sunspots tend form in groups or pairs and may last for several days, weeks, or even as long as two months.

The number of sunspots on the sun follows a 22-year cycle, with the number gradually increasing and decreasing during this time. During periods of high solar activity, Earth receives more radiation from the sun. Likewise, Earth receives less radiation from the sun during periods of low solar activity.

Over the past 124 years, Portland, Maine has received an average of 70.9 inches of snow per season. Fourteen of those seasons have seen a much higher amount - over 100 inches. Seven seasons have seen less than half that average, coming in with totals under 35 inches.

The hypothesis was that an analysis of seasonal snowfall amounts in Portland, Maine compared to the seasonal average of sunspots (October through May) would show a relationship between the two phenomena. It was believed that careful examination of the data would show a higher amount of snowfall during periods of low sunspot activity and a lower amount of snowfall during periods of high sunspot activity when the Earth was receiving more radiation.

OBSERVATIONS AND DATA REDUCTION

Sunspot numbers were gathered from the Sunspot Index Data Center according to monthly average. Because the numbers were going to be compared with seasonal snowfall amounts, and the snowfall season in Maine is from October until May, the average of sunspots for each month from October to May was added together and a seasonal average obtained.

Official monthly snowfall amounts for Portland, Maine were obtained from the National Weather Service in Gray, Maine. These monthly amounts from October through May were added together for all 124 years (1881-present).

The fourteen seasons in which Portland, Maine received greater than 100 inches of snow were then extracted from the data. The seasonal sunspot numbers (October through May) were entered into Microsoft Excel and graphed (see Figure 1). Likewise, the seasonal snowfall amounts for those fourteen seasons were also entered Microsoft Excel and graphed alongside the sunspot data. This made for easy comparison of the data.

A seasonal average of sunspots for all 124 years was also calculated and entered into the graph to provide a baseline for comparison. The graph was then analyzed to determine if, indeed, a relationship between seasonal sunspot number and snowfall amount in Portland, Maine exists.

ANALYSIS AND RESULTS

Figure 1. Average Sunspot Number and Snowfall Total for Years with 100+ Inches of Snow.

Winter Season	Seasonal average sunspot number	Seasonal amount of snowfall		Winter Season	Seasonal average sunspot number	Seasonal amount of snowfall
1883-84	130.54	118.0		1955-56	98.49	116.5
1886-87	9.56	125.5		1966-67	82.14	106.2
1898-99	18.32	115.3		1968-69	111.38	110.0
1906-07	57.77	119.5		1970-71	78.12	141.5
1922-23	6.21	125.0		1992-93	75.84	115.6
1933-34	6.3	119.1		1995-96	9.44	123.0
1951-52	35.96	105.0		2004-05	32.43	103.5

Figure 2. Average Sunspot Number and Snowfall for Years with less than 35 Inches of Snow.

Winter Season	Seasonal average sunspot number	Seasonal amount of snowfall		Winter Season	Seasonal average sunspot number	Seasonal amount of snowfall
1912-13	2.33	30.1		1979-80	166.3	27.5
1936-37	112.33	29.4		1990-91	139.28	32.4
1952-53	20.11	31.3		2001-02	115.7	32.6

Figure 3. Graph comparing seasonal average sunspot number with snowfall amounts for years when Portland, Maine received over 100 inches of snow.

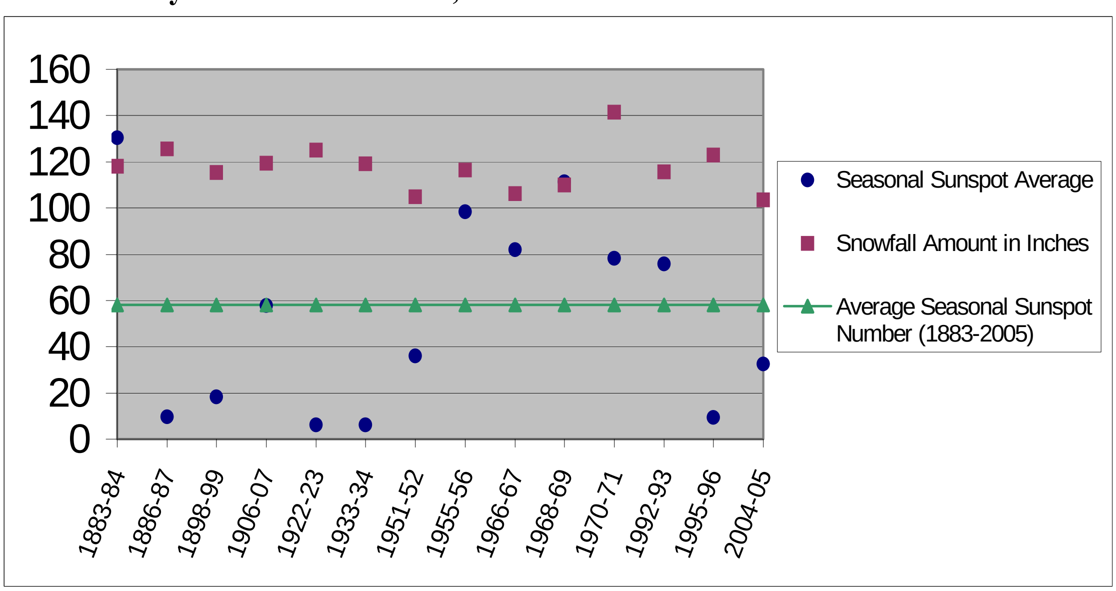

Figure 4. Graph comparing seasonal average sunspot number with snowfall amounts for years when Portland, Maine received less than 35 inches of snow.

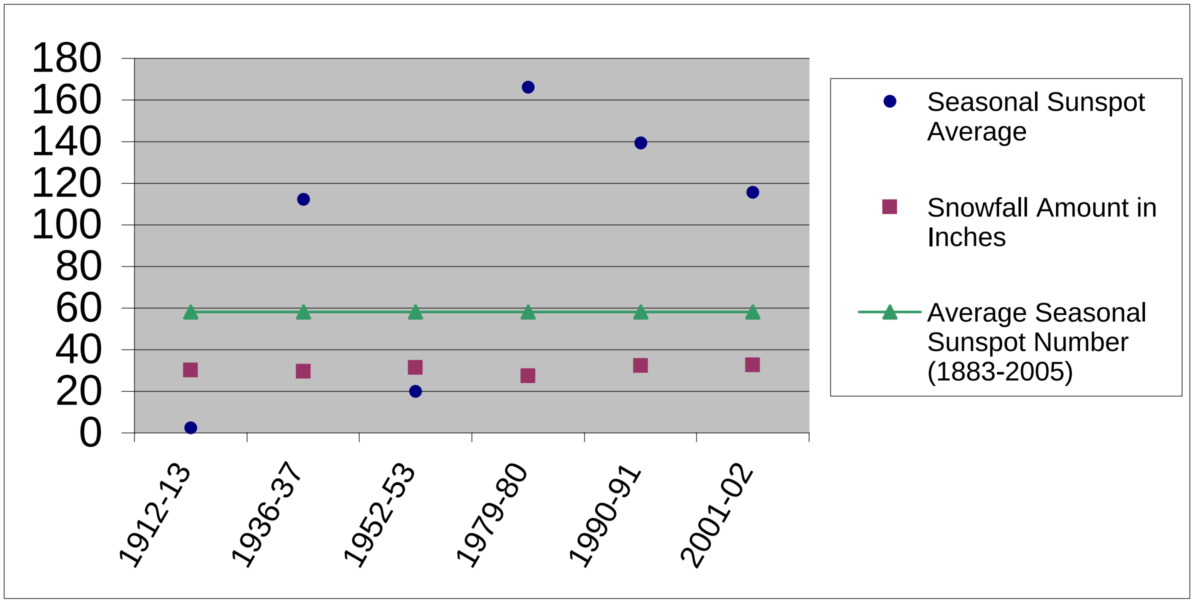

DISCUSSION

After comparing the data sets from the National Weather Service and from the Sunspot Index Data Center, it was determined that a definite relationship between seasonal average sunspot number and snowfall amount does not exist for Portland, Maine. Although other scientists have reportedly found a relationship in other regions of the Earth, the data for Portland, Maine did not support these claims.

The graph in Figure 3 shows that during the 14 years when Portland received snowfall amounts greater than 100 inches, 8 of those years had an average seasonal sunspot number that was lower than the total average. The other 6 years showed a pattern of sunspot activity that was greater than the total average, thereby disputing the theory.

While the graph in Figure 4 shows 4 of the 7 years of significantly lower snowfall amounts as being years of relatively high sunspot activity, it also shows 2 of those years as having substantially lower than average sunspot activity. Again, this disputes the theory that a pattern between the two phenomena exists.

While some scientists may look at this data and argue that a case for a relationship between seasonal average sunspot number and the amount of snowfall in Portland, Maine does exist, this scientist feels there is not enough definitive evidence to make that conclusion. Further study and analysis of data from other regions of the Earth may be needed in the future to make any definite conclusions of a global relationship.

SUMMARY AND ACKNOWLEDGEMENTS

Analysis of data from the National Weather Service and the Sunspot Index Data Center determined that a relationship between seasonal sunspot number and snowfall amounts in Portland, Maine does not exist. While some scientists have reported that they have found a relationship between these two phenomena in other regions, careful analysis of the data obtained for Portland did not support this theory. In the future, it may be necessary to obtain data from a variety of different regions around the world to get a global picture of whether or not a relationship may exist.

I wish to thank Chief Meteorologist Dave Santoro at WGME in Portland, Maine for assisting me in locating local snowfall data for the past 124 years. His help in connecting me to the data from the National Weather Service was instrumental in this study.

Furthermore, appreciation goes out to Don Robinson-Boonstra at NASA's Office of the Sun-Earth Connection at Goddard Space Flight Center for his assistance and inspiration during this project. His knowledge and expertise related to the sun were also a major factor in the success of this research.

Finally, this project would not be complete without acknowledging the staff of TLRBSE, especially Connie Walker, Steve Pompea, and Jeff Lockwood, who provided encouragement and support for this endeavor.

REFERENCES

www.sidc.oma.be/index.php3

http://son.nasa.gov

www.crh.noaa.gov/dtx/?page=winter2004-2005

www.gi.alaska.edu/snowice/snow1.html

www.erh.noaa.gov/er/gyx/climate.shtml

The Effect of Sunspot Size and Latitude on Magnetic Field Strength in Sunspots

Sarah Mullins and Sheena Stanley
Linwood Holton Governor's School
Dr. Steve A. Rapp, TLRBSE 2002

ABSTRACT
We conducted research to determine the magnetic field strength via Zeeman line splitting in infrared (IR) spectra for targeted sunspots of different sizes and latitudes. The unique infrared capability and large aperture of the McMath-Pierce telescope made it perfect for this type of study. We collected several data sets over a two-day period. Using computer programs KP and Image J, we reduced the data and determined the magnetic field strength of active regions on the Sun at that time. A total of three active sunspot regions were observed and reduced for further research. After reducing and analyzing the data we collected, we can say that size and latitude are factors in the magnetic field strength of sunspots. The greater the area of a sunspot, the greater the magnetic field strength is. The closer the sunspot is to the poles of the Sun, the greater the magnetic field strength is.

INTRODUCTION

We were 1,941 miles from home and 6,875 feet above sea level before we realized it was not just a dream. After researching for hours, writing a proposal, and conducting a few teleconferences, we were really at the Kitt Peak National Observatory. We were two students standing on a mountain made for research. A once in a lifetime opportunity stood before us, and we took full advantage of it. Our purpose was to research sunspots on the world's largest solar telescope (see Image 1) in hopes of learning more about the world of science.

We conducted research to determine the magnetic field strength via Zeeman Line Splitting in IR spectra for targeted sunspots of different sizes, latitudes, and intensities. The unique infrared capability and large aperture of the McMath-Pierce telescope made it perfect for this type of study. We collected several data sets over a two day period, December 2, 2004 through December 3, 2004. Using the "Data Reduction" and analysis ("KP") programs, we reduced the data and determined the magnetic field strength of active regions on the Sun at that time. With the Image J program, we determined the latitude and longitude range and the area for each sunspot. A total of three active sunspot regions were observed and reduced for further research.

Sunspots have been compared to low-pressure areas, tornados, or huge whirl winds in the solar gas. Complex movements of gas both into and away from a sunspot have been observed. Recent theories say that sunspots are cool areas produced by reactions between the charged gases of the Sun and solar magnetic fields. A local magnetic field breaks through the surface of the photosphere and produces a spot that place. They are cooler and less bright than the rest of the photosphere. The umbra, a dark central region of the sunspot, is 5 times less bright than the surrounding photosphere and so appears dark. The penumbra is the lighter surrounding area. At certain places near the edge of the Sun, the spots look like depressions in the photosphere. The intensity of the magnetic field strength would increase as you approach the umbra and decrease as it leaves the umbra (http://www.exploratorium.edu/sunspots/index.html).

The Zeeman Effect, or Zeeman splitting, is the splitting of spectral lines. It was named after Pieter Zeeman, a Dutch physicist. Zeeman Splitting can be used to study the magnetic field strengths of stars and sunspots. The Zeeman Effect can show variances in magnetic field strength, from weak fields with very little spectral line splitting to strong fields with a lot of spectral line splitting. (http://www.daviddarling.info/encyclopedia/Z/Zeemaneffect.html).

Image 1- McMath-Pierce Solar Telescope (photo by Sarah Mullins)

Our scientific motivation was multifaceted. First, we set out to prove our hypothesis, true or false. We set out to prove that the magnetic field strength of a sunspot becomes greater as the area of a sunspot increases; we also wanted to determine if the magnetic field strength of a sunspot was greater if it was closer to the poles of the sun. Second, we wanted to gain more experience with scientific research. Finally, our third objective was possibly to discover something unknown about sunspots. We felt that it was important to use our knowledge to learn more about the unknown and use all possible resources in doing so.

OBSERVATIONS AND DATA REDUCTION

To retrieve the information to conduct the research, we were privileged enough to use the world's largest solar telescope, the McMath-Pierce telescope. Infrared spectroscopy and imaging is one of its primary uses. On November 29 - 30, 2004, we used the 13.7-m Czerny-Turner solar spectrograph, which scans wavelengths, and utilizes an infrared camera called the Near Infrared Magnetograph (NIM). The infrared camera incorporating a 256 x 256 indium antimonide array detector can be used with the visible grating in the range 1 - 2.5 microns and for direct imaging over the range 1 - 5 microns. With this instrument we captured images of sunspots and took spectra of them at about 1.5 microns.

Using the NIM and its adaptive optics, we followed a process to retrieve the information. We locked on to active regions of the Sun and scanned across them (see Image 2). After the scan of each active region, we also had to obtain "darks" and "flats" scans. Darks and flats are used to subtract the instrumental "noise" and normalize the data (respectively). To do this, the data reduction program basically subtracts the darks from the data and divides the data by the flats. To obtain the dark scan, we closed the shutter. Next we had to take the flats. Simultaneously we stepped across the featureless part of the photosphere while scanning across the spectrum. This was in an effort to normalize both spatially and spectrally. After we had the scans, we were ready to start reducing and analyzing the data.

To reduce the data, we used the "Data Reduction" program on the Solar Data CD-ROM. We chose an image frame from the middle of the region, about 50. Then we chose a dark frame and a flat frame. Then we saved the results so we could view them later. We did the above process for each scan of each active region.

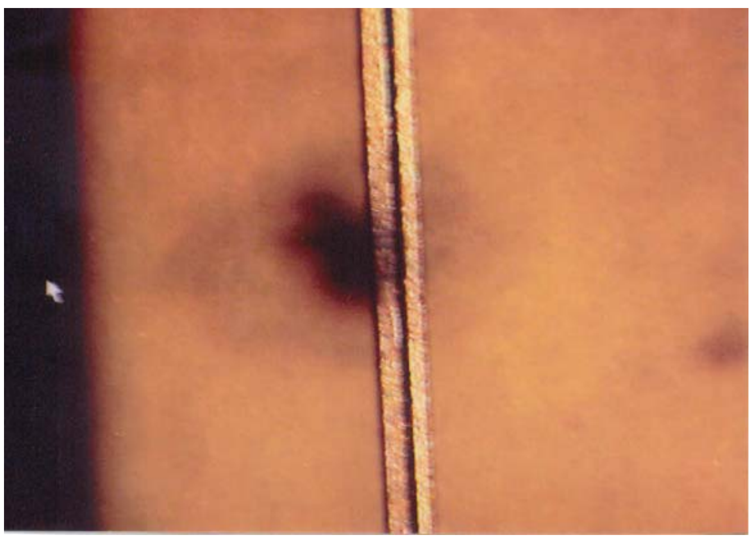

Image 2- Scanning Across the Sun (photo by Sarah Mullins)

Using the data analysis program called "KP", we then opened a spectra image (see Image 3) from the middle of the active region. We drew a small box around the central region of the umbra of one set of split spectral lines. Then we found the left, center, and right pixel location of the Zeeman lines. Then we calculated the differences between the center and left-hand point and between the right-hand point and the center. We converted the differences in pixel to differences in Angstroms by multiplying the pixel difference by 0.0825 Angstroms/pixel.

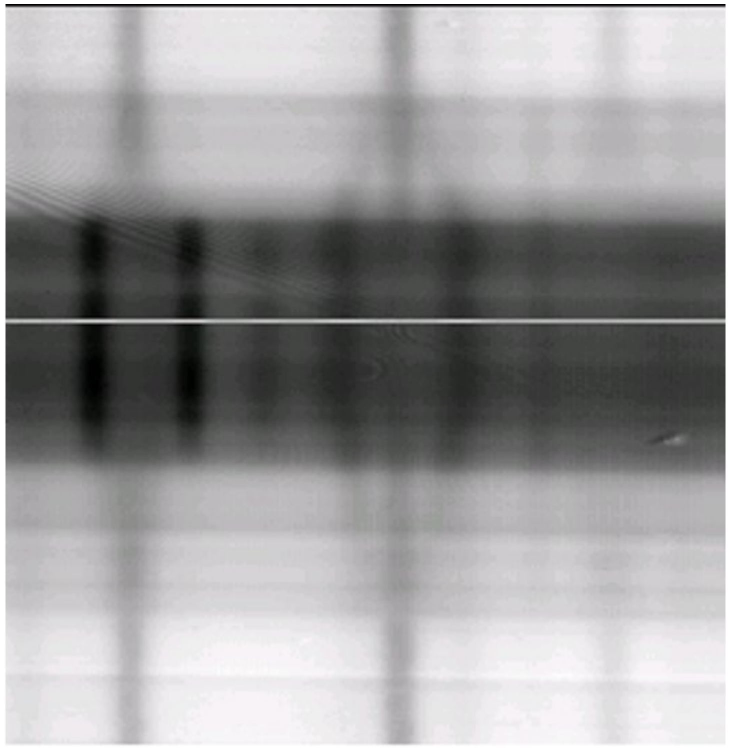

Image 3- Spectra Image of Zeeman Splitting (photo taken by Dr. Steve Rapp)

Using our Angstrom differences, we used the formula below to find the magnetic field strength in Gauss (see Table 1).

$$B = 2.13 \times 10^{12} [\Delta\lambda/(\lambda^2 \cdot g)]$$

We found the standard deviation for each scan of the active regions by taking the magnetic field strength from the right to the center minus the magnetic field strength from the center to the left. Using the standard deviation formula:

$$SD=sqrt \{\Sigma (x\text{-}mean)^2(1/n\text{-}1)\}$$

We found that possibility for error could be + or – 239.075 Gauss. To find the standard deviation, we added a pixel to the pixel difference from the central spectral line minus the left spectral line and used that value in the magnetic field strength equation. We then subtracted a pixel from the pixel difference from the central spectral line minus the left spectral line and used that value in the magnetic field strength equation. We took the larger of the two values that we found and subtracted the lesser value. We divided the difference between the two new magnetic field strength values by 2 to determine that the possible error for our magnetic field strength calculations is + or – 239.075.

Magnetic Field Strength of Sunspots (Calculated in Gauss) Error + or – 239.075 Gauss		
	Center Spectral Line - Left Spectral Line	**Right Spectral Line - Center Spectral Line**
Active Region 0706	**2151.66**	**2390.74**
Active Region 0707 Part A	**2868.89**	**2868.89**
Active Region 0707 Part B	**2390.74**	**2390.74**
Active Region 0707 Part C	**1673.52**	**1912.59**
Active Region 0707 Part D	**2151.66**	**1912.59**
Active Region 0708	**2390.74**	**2390.74**

Table 1- The Magnetic Field Strength of Active Regions 0706, 0707, and 0708

To make the spectroheliograms, we opened a reduced data file. We drew a box around the entire spectrum. Then the program processed the data and saved it. We were then able to view an image of our sunspots.

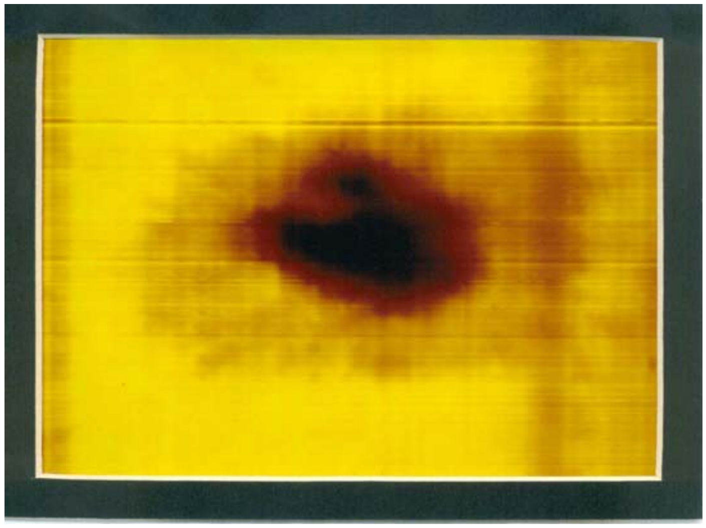

Image 4- A Spectroheliogram that we made of active sunspot region 0707A using the KP program

We used Image J to find the area of the active regions. To do this, we first retrieved a fits file from the Big Bear Solar Observatory (http://www.bbso.njit.edu/).We opened the file in Image J. Then we maximized the area by focusing on one active region and zooming in on it. We drew a box around the active region and adjusted to the threshold. We counted the pixel number across the Sun and found it to be 784. We know the diameter of the Sun is 1.4 million Km. We set the scale by using the above measurements. After finding the pixel distance across each sunspot, we converted that distance to kilometers. Using the kilometer measurements the sunspots, we calculated the area of each sunspot. With scan 0707, we found the area of each of the three smaller spots, the larger spot, and then added them together. After we calculated the area in kilometers, we converted our area measurements in astronomical units (see Table 2).

Sunspot Area In millions of km^2	
Active Region 0706	**331**
Active Region 0707A	**331**
Active Region 0707B	**31**
Active Region 0707C	**51**
Active Region 0707D	**76**
Active Region 0708	**527**

Table 2- The Sunspot Areas of Active Regions 0706, 0707, and 0708

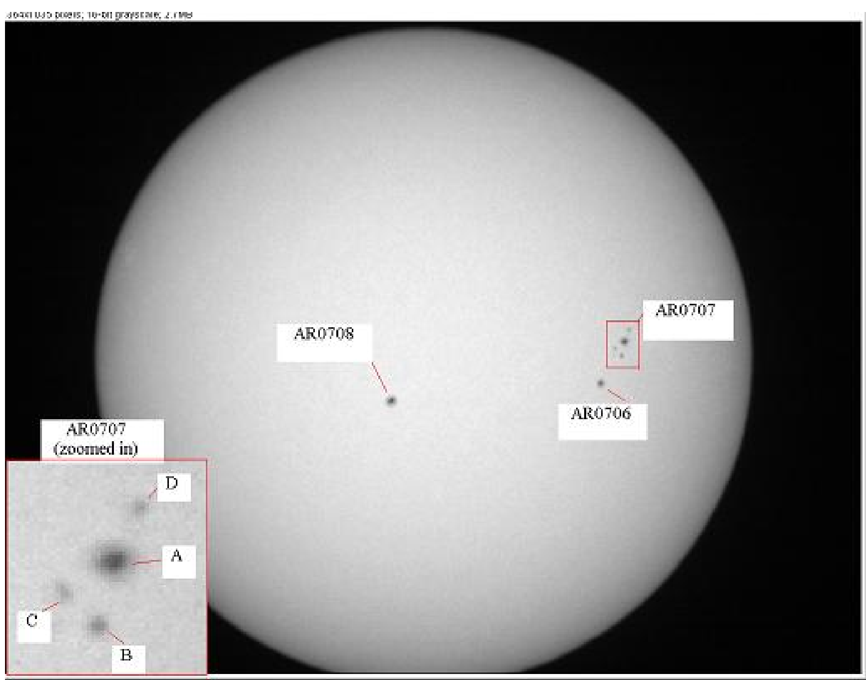

Image 5- jpg image from BBSO with labeled active sunspot regions

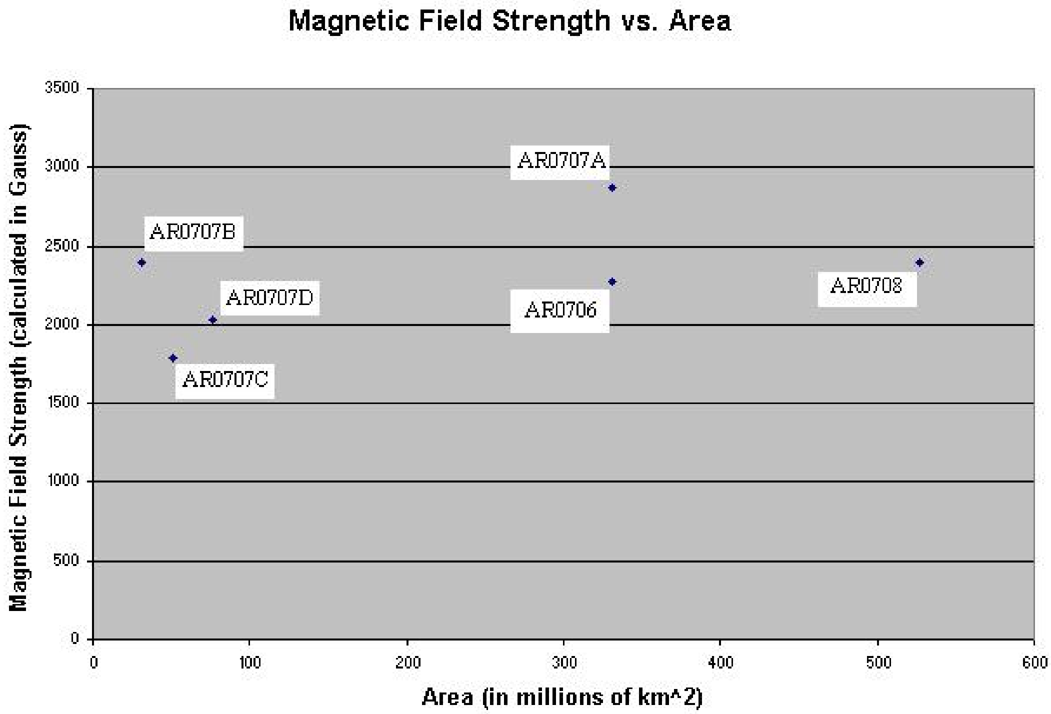

Graph 1- Magnetic Field Strength vs. Sunspot Area

In order to find the latitude and longitude of the sunspots we again used an image from the Big Bear Solar Observatory (http://www.bbso.njit.edu/). From the Big Bear Solar Observatory's daily files, we observe an image of the Sun that included latitude and longitude grids. We found the latitudes and longitude of the active regions according to that image (see Table 3).

Sunspot Location (In arc seconds)		
	Latitude	**Longitude**
Active Region 0706	**-116 to -25**	**330 to 460**
Active Region 0707A	**-290 to –250**	**550 to 590**
Active Region 0707B	**-230 to -215**	**570 to 590**
Active Region 0707C	**-250 to -230**	**540 to 555**
Active Region 0707D	**-320 to -290**	**560 to 580**
Active Region 0708	**-100 to 85**	**60 to 140**

Table 3- The Sunspot Location of Active Regions 0706, 0707, and 0708

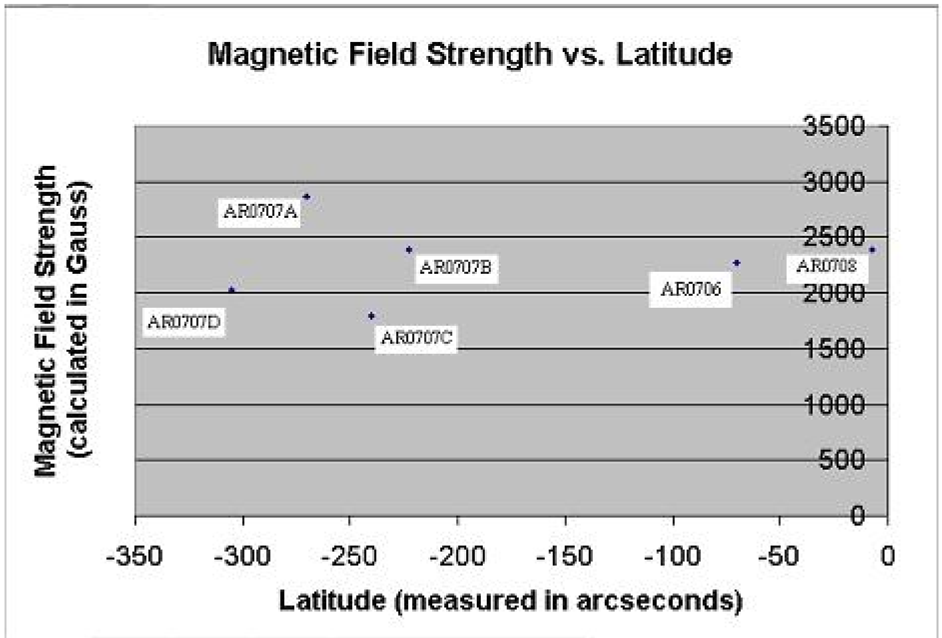

Graph 2- Magnetic Field Strength vs. Latitude (using average latitude and average magnetic field strength for each sunspot)

DISCUSSION

After reducing and analyzing the data we collected, we found that we could not definitely prove or disprove our hypothesis with undeniable certainty. The group of active sunspot regions that we collected and analyzed data for were moderately similar in size, latitude, and magnetic field strength; therefore, we were unable to determine if our hypothesis was correct or not. Upon comparing the latitude measurements and the magnetic field measurements, we found no negative or positive correlation between the two. The active sunspot regions with lesser areas did have somewhat lesser magnetic field strengths compared to the active sunspot regions with greater areas. However, the data that we analyzed was much too similar to make any conclusive decision on whether or not we could prove our hypothesis. More data from a larger range of areas and latitudes would have to be studied in order to undoubtedly prove or disprove our hypothesis.

SUMMARY AND ACKNOWLEDGEMENTS

Conducting this research at Kitt Peak was a once in a lifetime opportunity for us, and we would like to thank all of those who made it possible. We would like to thank our teacher, Dr. Steve Rapp for all of his help and guidance throughout our research. We would like to thank the Kitt Peak National Observatory for allowing us to come and use the McMath-Pierce Telescope. We would especially like to thank Connie Walker and all the other astronomers who helped us conduct our research. Lastly, we would like to thank the National Optical Astronomy Observatory and the National Solar Observatory for making this opportunity available to us.

REFERENCES

National Optical Astronomy Observatory [Online] Available at *www.noao.edu,* January 12, 2005.

"Sunspots: Introduction" [Online] Available at *http://www.exploratorium.edu/sunspots/index.html,* January 13, 2005

Big Bear Solar Observatory [Online] Available at *http://www.bbso.njit.edu/,* February 14, 2005

"Zeeman Effect" from *The Encyclopedia of Astrobiology, Astronomy, and Spaceflight* [Online] Available at htt*p://www.daviddarling.info/encyclopedia/Z/Zeemaneffect.html* January 13, 2005

Magnitude and Lifespan of Centered Galactic Novae vs. Outer Edge Galactic Novae

Eric Kalver and Anthony Petrocchi
Cranston High School East, Cranston, RI
Teacher: Howard Chun, RBSE 1999

ABSTRACT
The brightness and life of novae near the galactic center compared to the outer edge is the topic of research. It was predicted that the novae near the galactic center would be brighter and also have a shorter lifespan than the novae near the galactic outer edge. The sixteen subraster-fields of the M31 galaxy were observed, however, only five fields yielded novae. The novae's lifespan and magnitude in each field was observed, recorded, and graphed to form conclusions. Theory, and the results from previous studies, states that novae stars with a brighter magnitude will not live as long as those with a dimmer magnitude. Results from the data collected did show that novae from inner fields have a shorter lifespan than the novae in the outer fields. However, there was not enough data to truly support this conclusion or to make any other deductions concerning the comparison of magnitudes between inner novae and outer novae.

BACKGROUND
A nova is a faint star that rapidly becomes much brighter, sometimes 10,000 times more intense, and then fades over an extended period of time. Novae usually exist in a binary star system, in which two stars orbit about a similar point. The hydrogen from the second star becomes admitted into the first star. The hydrogen build-up eventually causes an explosion. The novae will eventually begin to fade again. Ultimately, the nova reaches the end of its life when it becomes a white dwarf (Adkins, D., et al, 2003). In other research projects, students discovered that novae with light curves of mower magnitudes decreased more rapidly, however, neglected to compare the magnitudes to their actual lifespans (Camacho, L., et al, 2001).

The images of the M31 used in the lab were taken with the KPNO 0.9-meter, MDM 1.3-meter, and the KPNO 2.1-meter telescopes at Kitt Peak National Observatory located in Arizona. The original images are large – 2048 x 2048 pixels. To make them easier for observation, each image has been divided into 16 subraster images or fields as shown below.

EXHIBIT

The Andromeda Galaxy Orientation of Fields:

1	*2*	*3*	*4*
5	*6*	*7*	*8*
9	*10*	*11*	*12*
13	*14*	*15*	*16*

The magnitude scale with which the brightness of stars are measured is read opposite of as what one may think. The magnitude scale is a logarithmic scale in which each integral step corresponds to a change of approximately 2.5 times in brightness. However, the smaller numbers correspond to brighter stars and the larger numbers correspond to dimmer stars. Thus a 1-magnitude star is brighter than a 2-magnitude

Astronomers measure the position of objects in the sky by imagining that these objects lay upon a celestial sphere, an imaginary hollow sphere inside which the Earth resides as the center. Two celestial coordinates, right ascension and declination describe the position of objects on the celestial sphere. The right ascension is analogous to longitude on earth while declination is analogous to longitude.

PURPOSE/QUESTION

Does a difference in magnitude and lifespan exist when comparing novae in the galactic center against novae in the galactic outer edge of the Andromeda galaxy?

HYPOTHESIS

A difference in magnitude will exist between the novae of the M31 galactic center and the novae of the M31 galactic outer edge. The novae near the galactic center would be brighter, thus giving off more energy and having a shorter lifespan that that of the novae in the galactic outer edge.

MATERIALS

- 1 Computer
- Vernier Graphical Analysis 3.1 for Microsoft Windows
- 1 RBSE CD-ROM
- Scion Image Program
- 1 M31 Data Sheet
- M31 Subraster/Field Images (with known magnitudes)
- Searching for Novae Lab Notebook – Data Chart

PROCEDURE

Scion Image was used to search for novae in sixteen fields of Andromeda in the M31 data files. Many images of the same area were viewed in search of disappearing and reappearing stars. This action is quite similar to a flipbook. Once the “spots” on the fields were confirmed to be novae, the magnitudes were measured and their life light curves were made. The life span of the novae can be estimated based on these measurements. The dates of the novae’s life were recorded on a spreadsheet, along with their magnitudes, using Microsoft Excel. The numbers were then graphed. The results that the graphs yielded were analyzed to form a conclusion.

DATA

Data of five out of sixteen fields from the M31 data files from the RSBE CD-ROM was collected. Fields 6, 7, & 11 were the inner fields and fields 5 and 14 were outer edge fields. The program, *Scion Image,* was used to view and analyze this data. Data of at least one nova in each field was composed. Field number 7 in particular yielded two novae. The novae lifespan was observed and recorded using it’s epoch date. *Scion Image* then calculated the novae’s magnitude based off of known magnitudes (which were given as part of the lab write-up) of the surrounding stars.

FIELD NO.	RA (hh:mm:ss.ss)	DEC (dd:mm:ss:ss)	EPOCH DATE (y/m/d)	MAGNITUDE	
5	.00:43:28.64	(+) 41:21:43.3	98/06/6	16.43	
5	.00:43:28.65	(+) 41:21:43.4	98/07/24	16.60	
5	.00:43:28.66	(+) 41:21:43.5	98/07/25	16.70	
5	.00:43:28.67	(+) 41:21:43.6	98/08/26	16.22	
5	.00:43:28.68	(+) 41:21:43.7	98/09/5	16.44	
5	.00:43:28.69	(+) 41:21:43.8	98/10/14	16.96	
5	.00:43:28.70	(+) 41:21:43.9	98/10/30	17.21	
5	.00:43:28.71	(+) 41:21:43.10	98/11/11	17.33	
5	.00:43:28.72	(+) 41:21:43.11	99/01/27	18.02	
6	.00:43:06.92	(+) 41:18:09.0	98/07/24	15.78	< DISREGARDED*
6	.00:43:08.35	(+) 41:16:40.6	95/09/3	15.82	< DISREGARDED
7	-	-	97/07/23	15.76	
7	-	-	97/07/24	17.87	<DISREGARDED
7	-	-	97/07/25	15.72	
7	-	-	97/07/31	16.00	
7	-	-	03/07/08	17.42	
7	-	-	03/07/09	17.34	
7	-	-	03/08/02	15.95	< DISREGARDED
7	-	-	03/08/03	15.88	< DISREGARDED

FIELD NO.	RA (hh:mm:ss.ss)	DEC (dd:mm:ss:ss)	EPOCH DATE (y/m/d)	MAGNITUDE	
7	-	-	03/08/30	17.36	
7	-	-	03/08/31	17.15	
7	-	-	03/09/17	17.80	
7	-	-	03/09/18	17.64	
7	-	-	03/09/19	17.70	
7	-	-	03/09/20	17.92	
7	-	-	03/09/21	17.77	
11	.00:42:31.1	(+) 41:15:35.5	03/08/02	16.21	< DISREGARDED
11	.00:42:38.6	(+) 41:14:18.4	97/06/18	14.23	<DISREGARDED
11	.00:42.32.0	(+) 41:14:42.2	97/07/23	15.79	
11	.00:42.32.1	(+) 41:14:42.3	97/07/24	16.10	
11	.00:42.32.2	(+) 41:14:42.4	97/07/25	15.88	
11	.00:42.32.3	(+) 41:14:42.5	97/07/31	16.17	
11	.00:42.32.4	(+) 41:14:42.6	97/08/1	16.12	
11	.00:42:39.6	(+) 41:15:27.8	99/06/24	15.72	< DISREGARDED
11	.00:42:39.7	(+) 41:15:27.9	99/07/20	16.66	< DISREGARDED
11	.00:42:22.1	(+) 41:11:31.6	98/10/14	16.79	
11	.00:42:22.2	(+) 41:11:31.6	98/10/30	17.11	
11	.00:42:22.3	(+) 41:11:31.7	98/11/11	17.52	
14	.00:42:57:14	(+) 41:07:17.7	00/11/11	17.03	< DISREGARDED * Data not used due to lack of relation to other data.

GRAPHS

Field 5

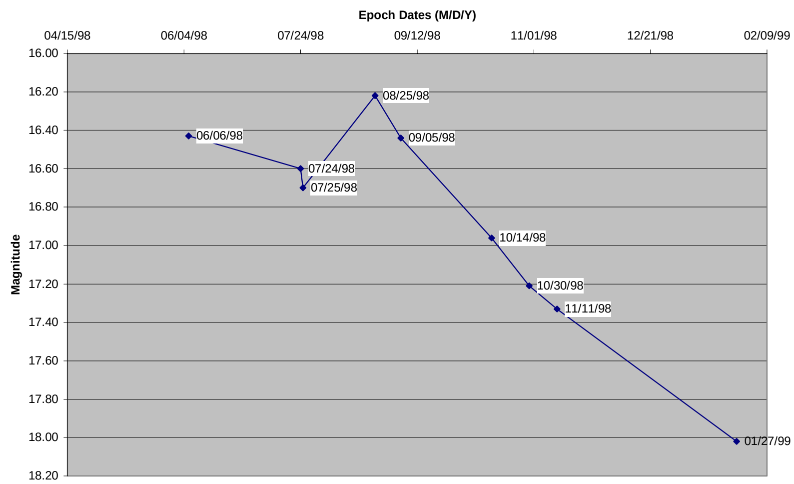

Field 7 (Nova A)

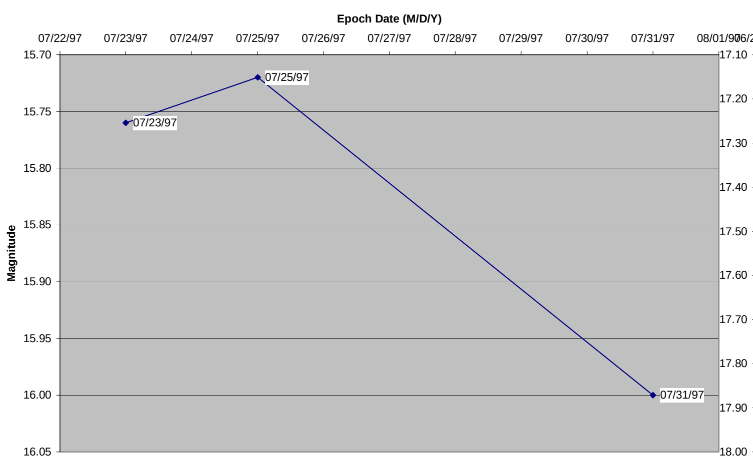

Field 7 (Nova B)

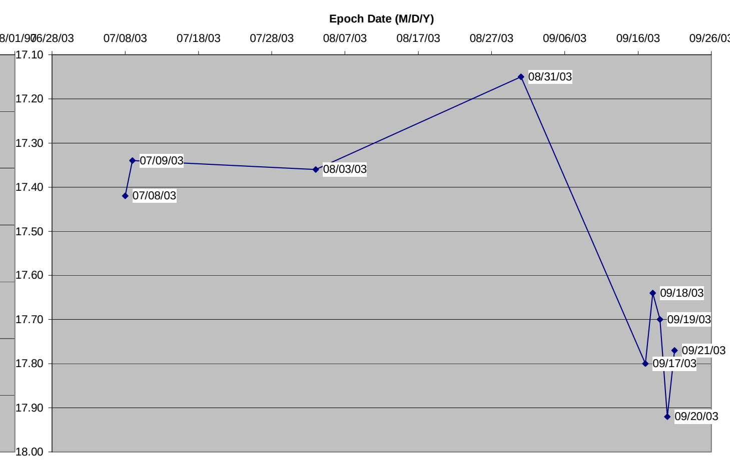

RESULTS TABLE

Field 11 (Nova A)

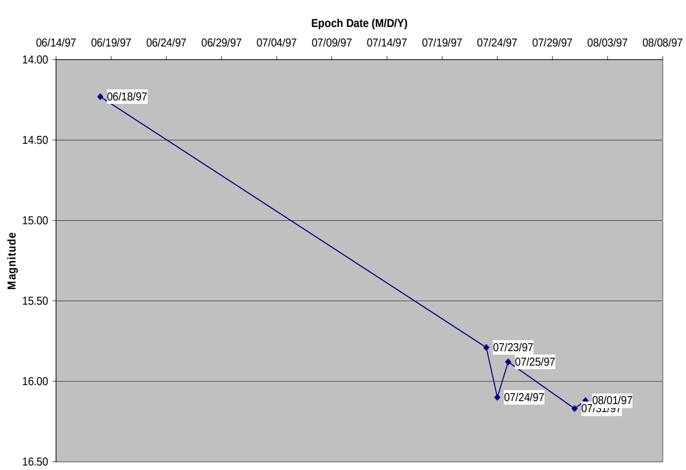

Field 11 (Nova B)

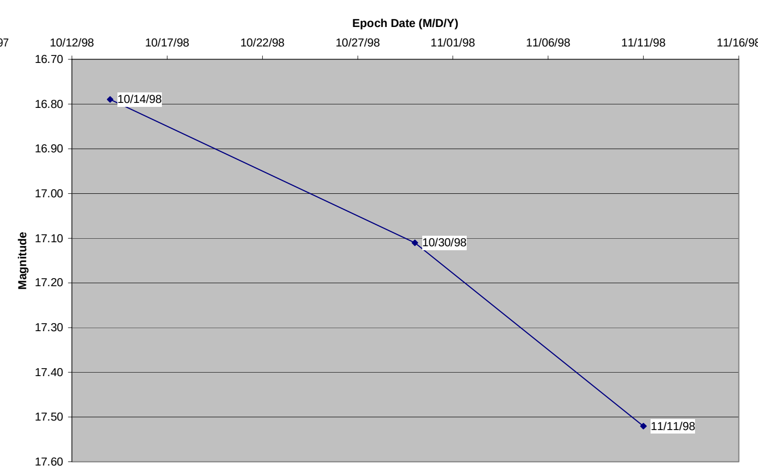

FIELD	EPOCH DATES	LIFE LENGTH	BRIGHTEST MAGNITUDE	DIMMEST MAGNITUDE
INNER	*FIELDS*			
7	97/07/23 - 97/07/31	8 Days	15.72	16.00
7	03/07/08 - 03/09/21	73 Days	17.15	17.92
AVERAGES		40.5 Days	16.43	16.96
OUTER	*FIELDS*			
5	98/06/06 - 99/01/27	231 Days	16.22	18.02
11	97/06/18 - 97/08/01	43 Days	15.18	16.17
11	98/10/14 - 98/11/11	27 Days	16.79	17.52
AVERAGES		**100.3 Days**	**15.75**	**17.24**

CONCLUSION

Previous endeavors of this experiment concluded that novae with a brighter initial magnitude seemed to have lifespans that decreased more rapidly than those that are not as bright (Camacho, L. et al, 2001). However, lack of sufficient data in this specific research project made for difficult and rather inaccurate conclusions. The data showed contrasting figures, which both supported and undermined our hypothesis. The results yielded that Field 7 (an inner field) had, on average, a longer day, a dimmer brighter-magnitude, and a brighter dimmest-magnitude compared to the outer fields in the M31 galaxy. The fact that the inner fields have a shorter day length than the outer fields supports our hypothesis. However, this idea contradicts the fact that the inner fields had a dimmer magnitude than the outer fields. In theory, these two measurements should correspond to each other – a brighter magnitude equals a shorter life and a dimmer magnitude equals a longer life. Thus, the experiment to determine whether the brightness and life of novae in the galactic center of Andromeda are brighter and shorter compared to the galactic outer edge was unsuccessful.

Due to the absence of an adequate amount of data, the results were scattered and insufficient to make an accurate conclusion. Undeniably, novae were much more common in the galactic center of the Andromeda galaxy. Many more novae were sighted in fields 6, 7, 10, and 11 than in the other remaining twelve fields, thus, supporting our hypothesis.

Since epochs were not taken in periodic intervals, the novae that only appeared in one epoch could not be could not be used in the lifespan study. This factor could have affected the results of this project, just as it has affected the outcome of other projects (Clark, N., 2003).

REFERENCES

Camacho, Linda and Miller, R. Magnitude of Novae in M31, RBSE Journal, 2001

Clark, Nick. The Lifespan of Novae in the Andromeda Galaxy, RBSE Journal, 2003.

Nova Search *Cosmic Easter Eggs* Packet (Revised: October, 1, 2001)
Travis A. Rector and George H. Jacoby

Adkins, Destinee. A Comparison of M31 Nova Rates to Other Spiral Galaxies, RBSE Journal, 2003

The Distance to M31 via a Cepheid

Barry G. Parker Jr.
Deer Valley High School, Antioch, CA
Teacher: Jeff Adkins, TLRBSE 2002

ABSTRACT

I found the light-curve of a Cepheid variable star in the Andromeda Galaxy with a period of 12 days and distance 1,227,229 light-years. This number was not right so after further analysis I discovered that this star was of the CW Virginis type of variable stars. The distance of this star as a CW is 2,554,400 light-years with an absolute magnitude of –5.97. This second number was much more in concurrence with the standard distance of 2.4 million light-years.

INTRODUCTION

I started this project searching for novas within M31 using data from the TLRBSE (Teacher Leaders in Research Based Science Education) research journal. The TLRBSE journal is a refereed journal of student research, also an outreach program for teachers and students. I thought that the star was a normal nova exploding; but after looking over different pictures taken over several years, I noticed that the star became dimmer then brightened again. The size of the star determines how much it dims and brightens; bigger stars are brighter. I asked my teacher about the blinking and he consulted Dr. Travis Rector (Adkins), who confirmed the blinking was a Cepheid variable, or a star that contracts and expands and changes its magnitude. Upon finding out that it is possible to find the distance to the star using its apparent and absolute magnitudes, I decided to find the distance to this star as a project.

HYPOTHESIS

By measuring the period relationship of a Cepheid type variable star within an astronomical body or alone, it is possible to find the distance to the object or the approximate distance to the body in which it is contained.

OBSERVATIONS AND DATA

I could not find the distance to this star via searching the Simbad and NED databases for stars. The databases are simply an online list of stars that the magnitude and locations are given. They contain information on thousands of stars, and many refer to them for this purpose of finding information. Below is a screen shot of the Simbad database. The method I used does work for finding distances, thus supporting my hypothesis. I found the distance to a specific Cepheid variable star in M31 at the location of Right Ascension 00:41:47.3 and Declination of +41:15:35.8 to be 1,227,229 light-years.

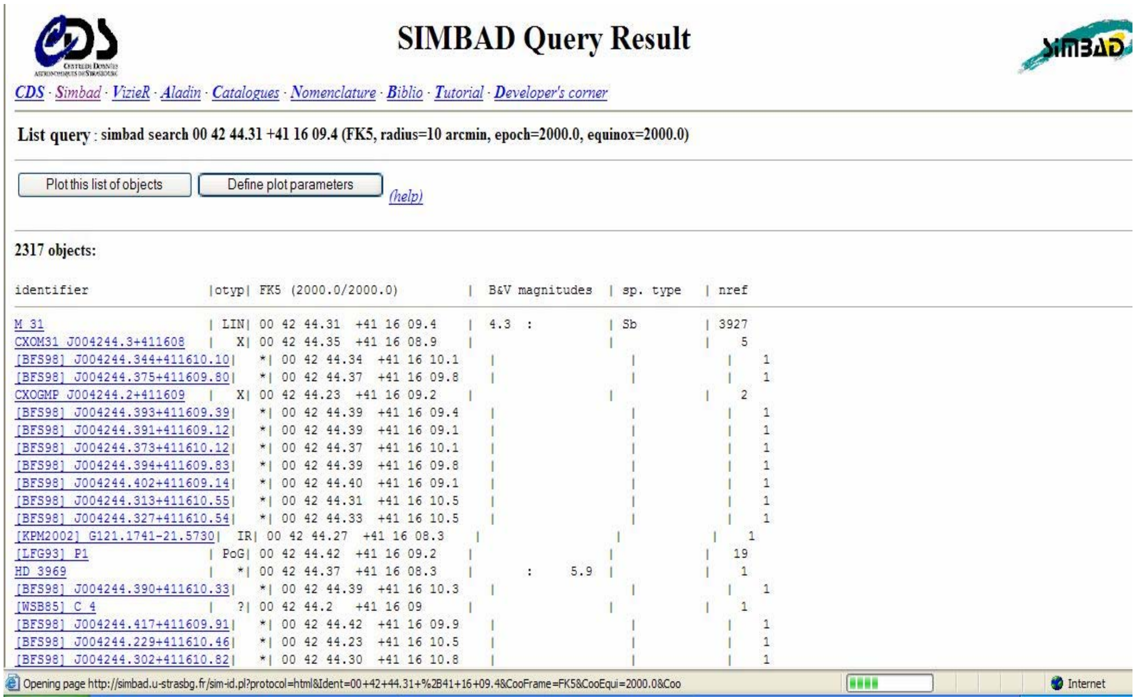
SIMBAD Query Result

CDS · Simbad · VizieR · Aladin · Catalogues · Nomenclature · Biblio · Tutorial · Developer's corner

List query : simbad search 00 42 44.31 +41 16 09.4 (FK5, radius=10 arcmin, epoch=2000.0, equinox=2000.0)

Plot this list of objects | Define plot parameters | (help)

2317 objects:

identifier	otyp	FK5 (2000.0/2000.0)	B&V magnitudes	sp. type	nref
M 31	LIN	00 42 44.31 +41 16 09.4	4.3 :	Sb	3927
CXOM31 J004244.3+411608	X	00 42 44.35 +41 16 08.9			5
[BFS98] J004244.344+411610.10	*	00 42 44.34 +41 16 10.1			1
[BFS98] J004244.375+411609.80	*	00 42 44.37 +41 16 09.8			1
CXOGMP J004244.2+411609	X	00 42 44.23 +41 16 09.2			2
[BFS98] J004244.393+411609.39	*	00 42 44.39 +41 16 09.4			1
[BFS98] J004244.391+411609.12	*	00 42 44.39 +41 16 09.1			1
[BFS98] J004244.373+411610.12	*	00 42 44.37 +41 16 10.1			1
[BFS98] J004244.394+411609.83	*	00 42 44.39 +41 16 09.8			1
[BFS98] J004244.402+411609.14	*	00 42 44.40 +41 16 09.1			1
[BFS98] J004244.313+411610.55	*	00 42 44.31 +41 16 10.5			1
[BFS98] J004244.327+411610.54	*	00 42 44.33 +41 16 10.5			1
[KPM2002] G121.1741-21.5730	IR	00 42 44.27 +41 16 08.3			1
[LFG93] P1	PoG	00 42 44.42 +41 16 09.2			19
HD 3969	*	00 42 44.37 +41 16 08.3	: 5.9		1
[BFS98] J004244.390+411610.33	*	00 42 44.39 +41 16 10.3			1
[WSB85] C 4	?	00 42 44.2 +41 16 09			1
[BFS98] J004244.417+411609.91	*	00 42 44.42 +41 16 09.9			1
[BFS98] J004244.229+411610.46	*	00 42 44.23 +41 16 10.5			1
[BFS98] J004244.302+411610.82	*	00 42 44.30 +41 16 10.8			1

Opening page http://simbad.u-strasbg.fr/sim-id.pl?protocol=html&Ident=00+42+44.31+%2B41+16+09.4&CooFrame=FK5&CooEqui=2000.0&Coo

Internet

Variables

Time	**Independent**
Magnitude	**Dependent; what is being measured**
Distance	**Dependent; determined by magnitude**

Equipment

MAC/PC	**For viewing and measuring the magnitude**
NIH / Scion Image	**Software used in finding the magnitude**
Fathom	**Used in creating Time VS. Magnitude graph**
Telescope	**0.9 meter At Kitt Peak**
Camera	**CCD**
TLREBSE	**Source of all nova information and pictures**

I began to work on the files of the Cepheid, which are located in the TLRBSE journal data for finding novas. Analyzing each picture was time consuming. This was due to the volume of files that I had to process. The results are listed in the table below (See Fig. 1). In the end, this technique was like analyzing seventy-five pictures instead of a simple twenty-five.

PROCEDURE

I opened NIH Image for Mac (at school) and Scion image for PC's (at home) and loaded the appropriate nova search macros.

The + is the target star

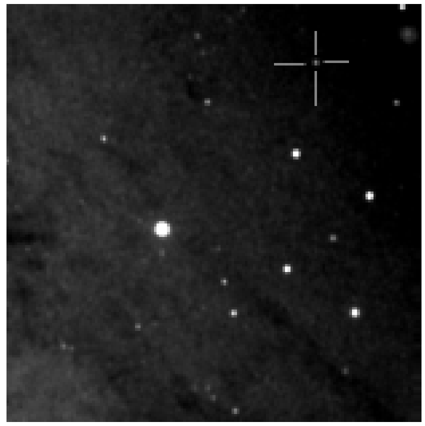

After loading the macros that were provided by TLRBSE, I opened the FITS files that contained the Cepheid in which I intended to measure.

Using a list of standard stars, I entered the magnitudes of them using the "Record Known Magnitude" function.

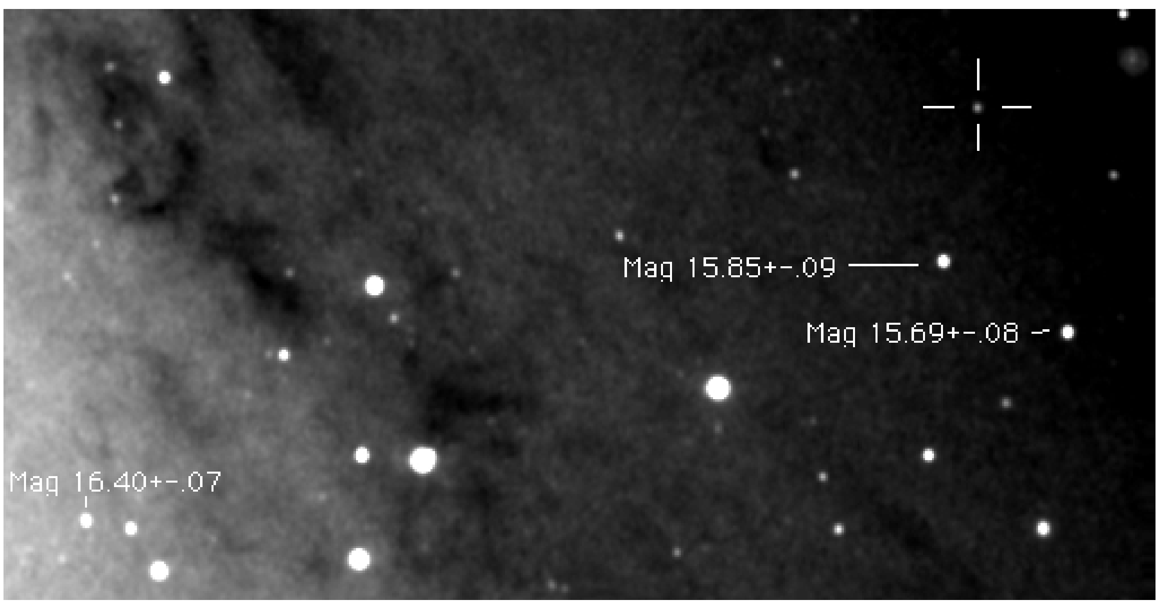

Upon inputting the known magnitudes, I used the "Measure Magnitude" button to find the magnitude of the star. I used the magnitudes of the other stars in order to establish a base against which I could measure the Cepheid variable. These were called Standard Stars.

I repeated this process for all the FITS files.

After recording all the magnitudes, I made a spreadsheet and entered all the converted Julian Dates with their corresponding magnitude measurement. A Julian Date is the date in numerical form starting from the day 0 to the present.

To convert the days to the Julian calendar date I used a program found on the web provide by the US Naval Observatory (http://aa.usno.navy.mil/data/docs/JulianDate.html).

Fig. 1

File/Picture	Magnitude	Date Taken	Julian Date
1	17.85	September 3 1995	2449963.5
2	17.49	July 18 1997	2450647.5
3	17.63	July 23 1997	2450652.5
4	17.63	July 24 1997	2450653.5
5	17.55	July 25 1997	2450654.5
6	17.66	July 31 1997	2450660.5
7	17.69	August 1 1997	2450661.5
8	17.93	November 18 1997	2450770.5
9	19.25	June 6 1998	2450970.5
10	19.27	July 24 1998	2450988.5
11	*15.99*	*July 25 1998*	*2450989.5*
12	*15.36*	*August 26 1998*	*2451051.5*
13	19.00	September 5 1998	2451061.5
14	18.77	October 14 1998	2451100.5
15	18.40	October 30 1998	2451116.5
16	18.70	November 11 1998	2451128.5
18	17.88	January 24 1999	2451202.5
17	18.17	January 27 1999	2451205.5
19	17.97	July 20 1999	2451379.5
20	19.47	June 14 2000	2451709.5
21	19.63	July 17 2000	2451742.5
22	18.99	September 13 2000	2451800.5
23	19.02	September 14 2000	2451801.5
24	18.57	October 15 2000	2451832.5
25	*17.89*	*November 10 2000*	2451969.5
59	*18.24*	19 Sep 2003	2452901.5
60	*18.18*	20 Sep 2003	2452902.5
61	*18.29*	21 Sep 2003	2452903.5
62	*18.36*	9 Oct 2003	2452921.5
63	*18.44*	13 Oct 2003	2452925.5
65	*19.02*	5 Dec 2003	2452978.5
67	*19.04*	10 Dec 2003	2452983.5
68	*19.16*	11 Dec 2003	2452984.5
69	*19.03*	13 Dec 2003	2452986.5
70	*19.04*	3 Jan 2004	2453007.5
71	*19.06*	6 Jan 2004	2453010.5

The italic/bold entries have been removed from the graph due to errors in the file from which they were acquired.

After making a best-fit light curve, I used it to find the period of the Cepheid. (See Fig. 2)

Figure 2

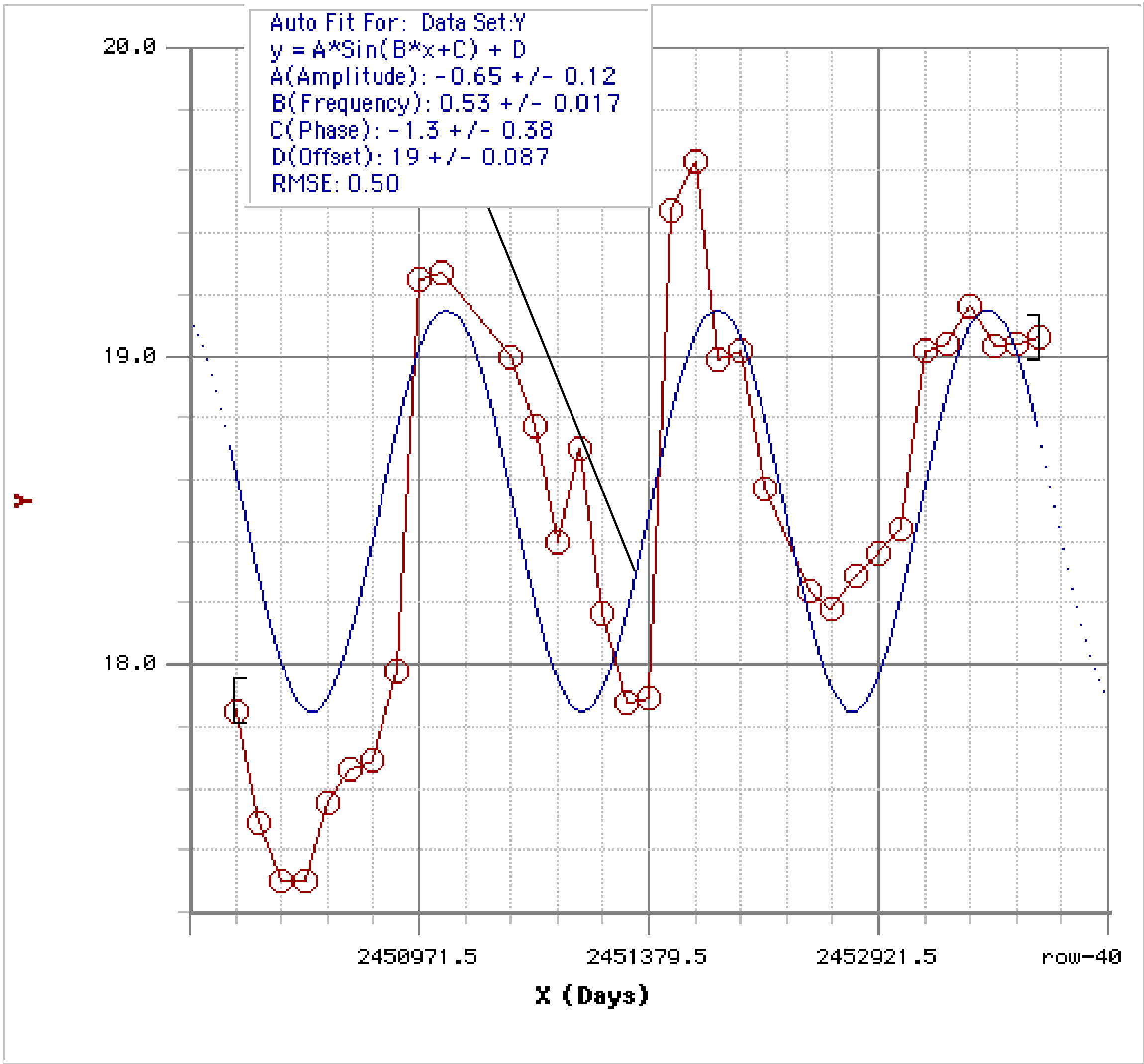

From this graph, I was able to extract a period of 12 days. The period is the distance between either two valleys or two peaks. In addition, from the graph the apparent magnitude was provided. The apparent magnitude is how bright we see the star on Earth. This number was simply the average of all the magnitudes of the star. These numbers are needed for finding the absolute magnitude or the brightness of the star if it were ten parsecs away. A parsec is an unit of measurement in astronomy equal to 3.26 light-years.

To find the absolute magnitude I used the equation below:

$M_v = -2.76(\log(P) - 1) - 4.16$ P= period or 12 days

$\mathrm{M_v} = -2.76(\log(12) - 1) - 4.16$

$\mathrm{M_v} = -2.76(.0791) - 4.16$

$\mathrm{M_v} = (-.2185) - 4.16$

$\mathrm{M_v} = -4.3785$

After finding the absolute magnitude, I was able to find the distance to the star using another astronomical equation:

$d_{pc} = 10^{((m - M_v + 5)/5)}$

$d_{pc} = 10^{((18.5-(-4.378)+5)/5)}$

$d_{pc} = 10^{((27.878)/5)}$

$d_{pc} = 10^{5.575}$

$d_{pc} = 376{,}450.64$

This distance comes out in parsecs in order to change it to light-years it is multiplied by 3.26.

$d_{ly} = 3.26(d_{pc})$

$d_{ly} = 3.26(376450.64)$

$d_{ly} = 1{,}227{,}229$

DISCUSSION

The period of this star according to the data I acquired is about 12 days. The Absolute magnitude is –4.378; for comparison, the Sun has an absolute magnitude of -27. The overall distance to the object in parsecs is 376,450 and the distance in light-years is 1,227,229.

Calculating reasonable numbers using this process confirms my hypothesis that it is possible to find the distance to the object by way of a Cepheid variable star. The real distance to the object M31 is 2-3million light years depending on the source.

Now as for my answer, it is off from what the given distance to the Andromeda Galaxy. I at first thought this answer was correct. I then discovered that there are two types of Cepheid variables (Strobel). The first is the classical type, which I first thought this star to be. I now think it is a CW of the Virginis type (This hypothesis is supported by the shape of the light curve. It contains a characteristic of this type of Cepheid in that it has a slight bump on its downward slope of the sine curve.)

If this hypothesis were true then the star would be four times fainter than it really is and thus twice as far from us. To test this I did the needed calculations. In order to make this star four times brighter the star it would be a difference of 1.59 magnitudes. Since 1 magnitude is 2.512 times brighter then 4 magnitudes is as follows:

$$M_{diff} = 4/2.512$$
$$M_{diff} = 1.592$$

Subtract this from the previous absolute magnitude and the answer is equal to the real absolute magnitude if it were a CW of the Virginis type.

$$M_{vNew} = M_v - M_{diff}$$
$$M_{vNew} = -4.378 - 1.592$$
$$M_{vNew} = -5.97$$

Again, I use this value in an equation to find the distance. Then multiply this answer by 3.26 to find the light-years of the star.

$$d_{pc2} = 10^{((m - M_v + 5)/5)}$$
$$d_{pc2} = 10^{((18.5 - (-5.97) + 5)/5)}$$
$$d_{pc2} = 10^{(29.47/5)}$$
$$d_{pc2} = 10^{5.894}$$
$$d_{pc2} = 783{,}558.34$$
$$d_{ly} = 3.26(d_2)$$
$$d_{ly} = 3.26(783558.34)$$
$$d_{ly} = 2{,}554{,}400$$

SUMMARY AND ACKNOWLEDGEMENTS

So overall this second answer is within the agreed distance to the galaxy and seems much more reliable than the first. This supports my theory that this star is not a Classical type Cepheid. That one fact accounts for many of the errors that were generated in this experiment.

The method as described in the first half of this paper does work for finding distances supporting my first hypothesis. The second hypothesis is supported in that that process gives an agreed on distance to the galaxy and a sensible distance for the star.

REFERENCE

Adkins, Jeff. "Possible Cepheid." E-mail to Dr. Travis Rector. 20 Apr. 2004.

Julian Date Converter. 14 July 2004. U.S. Naval Observatory. 20 Nov. 205 <*http://aa.usno.navy.mil/data/docs/JulianDate.html*>.

Silver, Samuel. Measuring Distance. N.p.: TERC, 1997. 2-36.

Stobel, Nick. Atronomy Notes. 4 Mar. 2005. 7 Apr. 2005 <*http://www.astronomynotes.com*>.

TLRBSE. TLRBSE. 3 Feb. 2005 <*http://www.noao.edu/outreach/tlrbse/*>.

Nova Rate in M31 Galaxy

Liz Herndon and Sarah Green
Graves County High School, Mayfield, KY
Teacher: Velvet Dowdy, TLRBSE 2003

ABSTRACT
This project is a study of the nova rate in M31, the Andromeda Galaxy, and a comparison of the nova rate in the inner fields versus the outer fields. Previous research has identified a controversy as to the location of the majority of nova in M31 and other galaxies. Should nova be found most often in the central bulge or the spiral arms? The results of this study indicate that the nova rate in the inner field is greater than that of the outer fields in M31.

Using images taken by the .9m telescope on Kitt Peak in Tucson Arizona, nova were found by "blinking" images of the same field throughout 75 epochs of data. Andromeda has to be imagined in 16 separate fields and an epoch is a night of observing. With this approach, new nova could be found and their location noted. The nova rate for each field was calculated and the rates were compared.

INTRODUCTION
The research question explored in this project was, "What is the nova rate in the inner fields compared to the outer fields of the Andromeda Galaxy?" This project is a study of the nova rate in the Andromeda galaxy, which is divided into subcategories comprised of four inner fields and twelve outer fields (Davidge 1992). "The Andromeda Galaxy" (also known as Messier Object 31, M31, or NGC 224) is a giant spiral galaxy in the Local Group, together with the Milky Way galaxy (Wyse 2002). It is at a distance of approximately 2.9 million light years or 920 kpc, in the direction of the constellation Andromeda (Wales; Sanger 2001). Novae are the result of the sudden brightening of a white dwarf caused by the explosion of accumulated hydrogen gas on the surface (NASA's Observatorium 1999). Previous research had already divided the Andromeda Galaxy into inner and outer fields. It is an accepted theory that there will be more nova productivity in the inner fields. After looking at previous research involving nova rate in the Andromeda galaxy, it was decided that the group should compare the inner field rates and the outer field rates to determine which area had a higher nova productivity rate.

OBSERVATIONS AND DATA REDUCTION
The research of nova rate in the Andromeda Galaxy was conducted using Scion Image. The images of Andromeda Galaxy were taken by the 0.9m telescope on Kitt Peak, near Tucson, Arizona. These images were made available through a TLRBSE (Teacher Leaders in Research Based Science Education). This program is funded by National Optical Astronomers Organization (NOAO), National Science Foundation (NSF), and the Association of Universities for Research in Astronomy (AURA). The research involved each group member "blinking" different sets of nova (Cardenas, Gloria 2002). "Blinking" is a way in which nova was categorized into different epochs then grouped into different fields (Hubble 1998). The Andromeda Galaxy is divided into 16 fields because it is so big viewing of the whole galaxy at once is not possible. Each group member was assigned

four different fields, because there were sixteen total with only four group members (Image 1). Each field contained 75 epochs that were examined individually and compared to each other. An epoch is a night that the Andromeda Galaxy was viewed. Epoch one was compared with epoch two, then epoch two was compared to epoch three, and so on. The comparison between epochs was formatted into a table. With this approach, the group could record each time a new nova appeared and where it was located.

Diagram 1
Andromeda Galaxy

1	**2**	**3**	**4**
5	**6**	**7**	**8**
9	**10**	**11**	**12**
13	**14**	**15**	**16**

This diagram represents how the Andromeda Galaxy is divided up into 16 fields. Fields 1-5, 8, 9, and 12-16 are called the outside fields. Fields 6, 7, 10, and 11 are the inner fields.

There were 118 total number of novas found in the four inner fields. The novas in the M31 were viewed over a time-period of 10.214 years (Rector, 2004). To find the nova rate divide 118 (total number of novas) by 4 (fields) and then divide by 10.214 (years that M31 was viewed). The nova rate for the inner fields was 2.888 novas per year.

In the twelve outer fields, a total number of 184 novas were found. The novas in the M31 were viewed over the same time-period of 10.214 years (Rector, 2004). The outer field nova rate was calculated by dividing 184 (total number of novas) by 12 (fields) and then dividing by 10.214 (years that M31 was viewed). The nova rate for the outer fields was 1.501 novas per years.

ANALYSIS AND RESULTS

Calculations
Nova Rate in M31

Inner Fields	Outer Fields
118 total novae found	184 total novae found
4 fields	12 fields
10.214 years of M31 epochs	10.214 years of M31 epochs
Rate= 2.888 novae/year	Rate= 1.501 novae/year
118/4/10.214= 2.888	184/12/10.124= 1.501

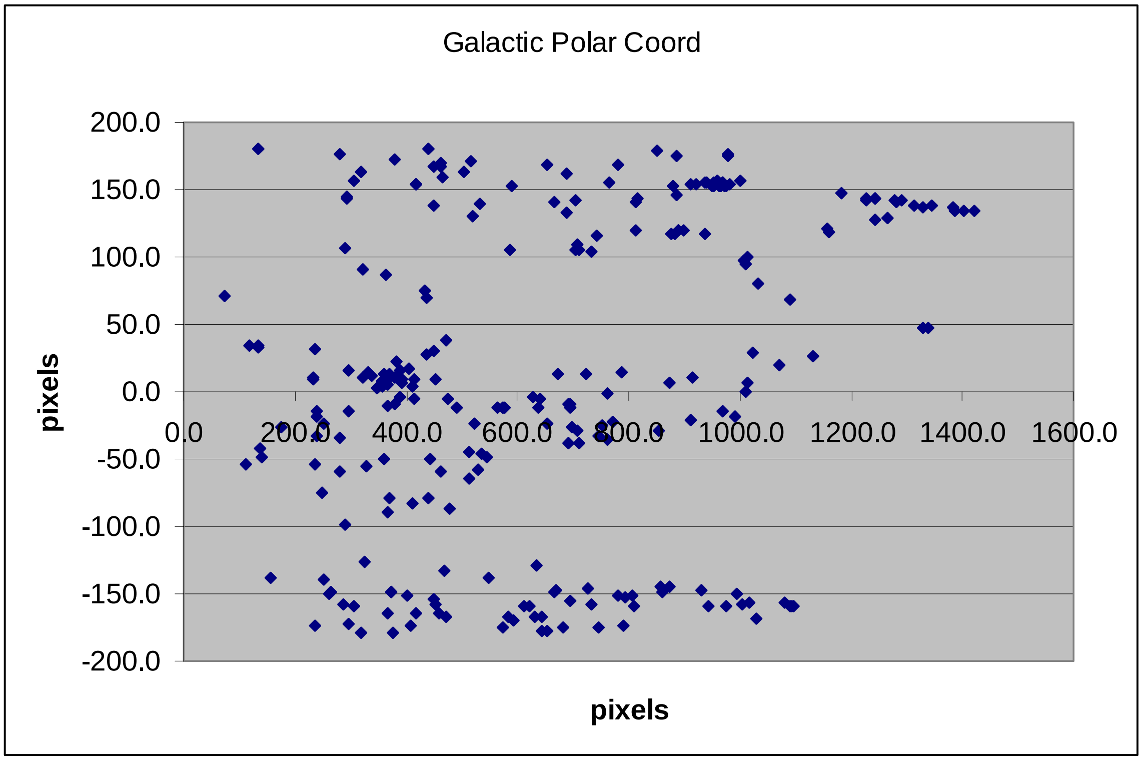

This graph shows the distribution of nova based on galactic coordinates.

DISCUSSION

The initial research question was to compare the nova rates of the inner and outer fields of the Andromeda galaxy. The hypothesis stated that the rate of the inner fields would be greater than the rate in the outer fields (Arcetri 1999). In this study of the Andromeda (M31) Galaxy's Nova Rates, it was revealed that the nova rate in the inner fields is greater than that of the outside fields. The rate of inner fields was 2.888 novas per year, whereas the rate of the outside fields was 1.501 novas per year. The inner rate is almost two times the rate of the outer fields. One reason for the increased inner rate is that the galaxy is denser in the inner fields. More nova productivity occurs in the inner fields where the center of the galaxy is located.

There were some problems with the data not containing all the epochs. Some of the images looked as if they had parts missing, especially in the outer fields. When data was downloaded from the NOAO ftp site, epochs 62 through 70 were missing and not available for this study. The nine missing epochs in the M31 software could possibly change the results. In addition, the epochs were not recorded consistently. Some epochs were only days apart, and others many months or years. Due to the erratic spacing of the epochs it is possible that nova events were missed that could also alter the results.

SUMMARY AND AKNOWLEDGEMENTS

The conclusion was that the nova rate of the inner fields of the Andromeda Galaxy is greater than the outer field's nova rate. The inner fields have a much higher amount of nova productivity per year than the outer fields (Davidge 1993). Therefore, the hypothesis was correct.

The group would like to thank the following people: Mrs. Nance and the Graves County High School computer lab for allowing the group to work and providing copies of software and data disks, Mrs. Herndon for allowing space to work in her home and providing refreshments, Travis A. Rector for providing information on the M31 project, NASA ADS, National Optical Astronomy Observation, Association of Universities for Research in Astronomy, and National Science Foundation.

REFERENCES

Arcetri, Roma; Padova & Trieste Observatories; "Nova Theory"; January 29, 1999; *http://lbc.mporzio.astro.it/Documentation/Science/node38.html*

Cardenas, Gloria Marie; "The Quest for Novae in the Core of M31"; 2002; p21-23 *http://www.noao.edu/outreach /tlrbse/rbsejournal02.pdf*

Davidge, T.J.; "Imaging of Fields in the Inner Halo and Outer Disk of M31"; The Astrophysical Journal; May 20, 1993

Davidge, T.J.; "Novae in M31 Discovered with Wide-field Telescopes in Crimea and Latvia"; Astrophysics and Space Science; August 14, 1992

DeVore, Harlan, Dowdy, Velvet, Moran, Tom, and Sampson, Gary, "Mass Distribution of Nova in M31", RBSE Journal, 2004, *www.noao.edu/outreach/tlrbse/rbsejournal04.pdf*

Hubble, Alex; Krugler, Julie; Walton, Margaret; 1998 *www.noao.edu/outreach/tlrbse/rbsejournal03.pdf*

NASA's Observatorium; 1999; *http://observe.arc.nasa.gov/nasa/space/stellardeath/stellardeath_4a.html*

Rector, Travis A; "KPNO/WIYN M31 Data"; November 2004

Wales, Jimmy; Sanger, Larry; Wikipedia, The Free Encyclopedia; January 15, 2001; *http://en.wikipedia.org/wiki/Andromeda_galaxy#General_information*

Wyse, Rosemary; "M31, M33, and the Milky Way"; April 11, 2002; *http://arxiv.org/abs/astro-ph/0203190*

Redshifts of Starburst and Elliptical/Radio Galaxies

Joseph Dublin, Mark Ashley, Josh Keeling
Graves County High School, Mayfield, KY
Teacher: Velvet Dowdy, TLRBSE 2003

ABSTRACT
In this research project, the redshifts of starburst and elliptical and radio galaxies were studied. After looking at the spectra and finding the redshifts of each, it was then that the comparison of the two groups began. It was found that the redshifts of starburst galaxies were somewhat smaller than the redshifts of elliptical or radio galaxies.

INTRODUCTION
A redshift is a shift in the frequency of a photon toward lower energy or longer wavelength. It is defined as being a change in the wavelength of light divided by the light wavelength at rest (Redshift Information Guide, 2005).

A starburst galaxy is a galaxy that forms stars at a continuous rate. Starburst galaxies generally have strong emission lines with little to no absorption lines. They also lack a strong calcium break between 4000 and 5000 angstroms. (Rector, 2001)

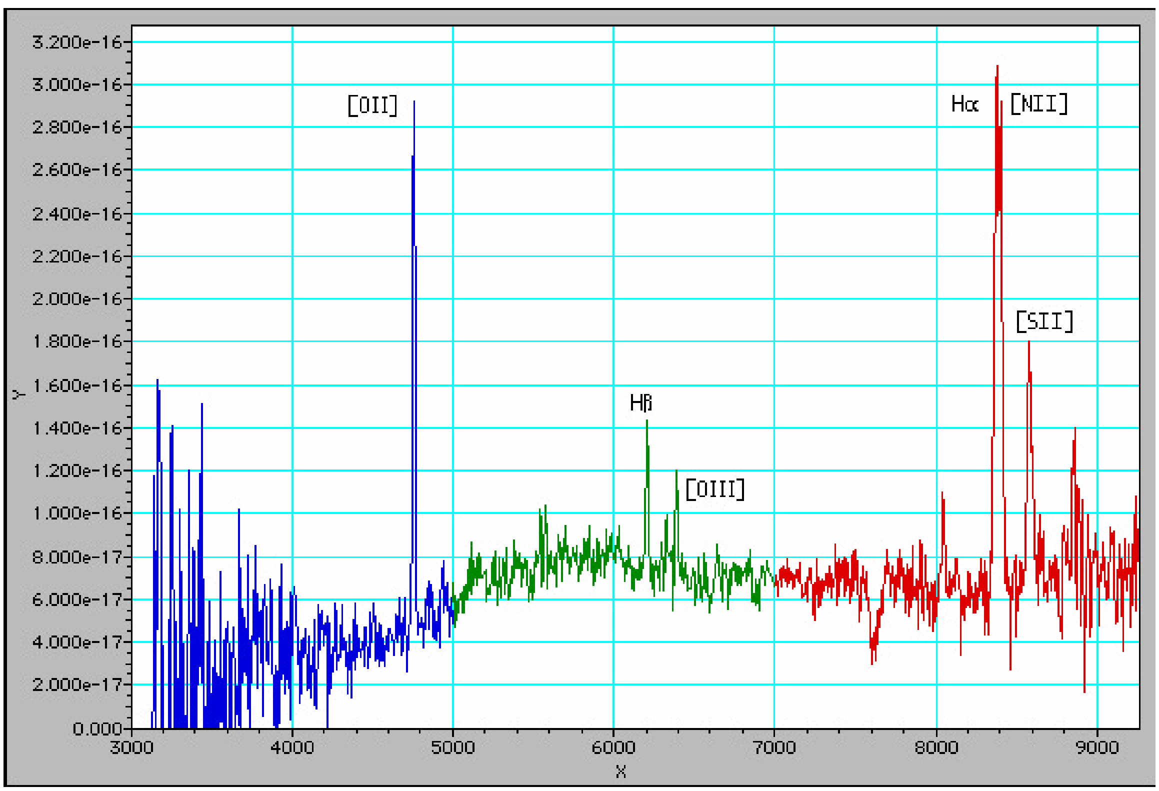

Starburst Galaxy (Rector, 2001)

Elliptical galaxies are very different from starburst galaxies. They are mainly composed of older stars and can either be very small or very large. They have a large Ca break between 4000-5000 Angstroms. (Rector, 2001).

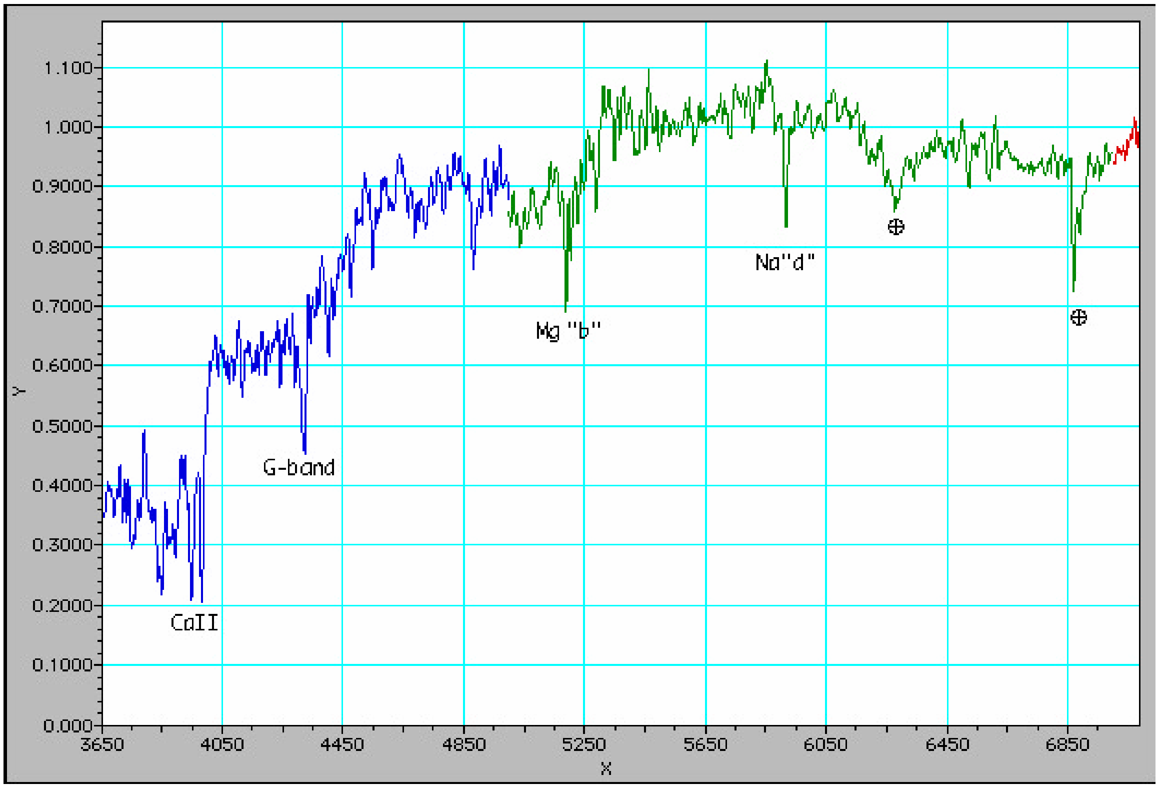

Elliptical Galaxy (Rector, 2001)

Radio galaxies have a small calcium break between 4000 and 5000 angstroms. The spectra of radio galaxies are very jagged with mid-range emission and absorption lines. They are easily distinguishable from elliptical and starburst galaxies. (Rector, 2001)

Our research question evolved from an unpublished paper of a previous year. In that study, the researchers attempted to find a difference between the distance of radio and elliptical galaxies from Earth. Our research question, formed from this prior study became and investigation of the difference between the redshifts of elliptical/radio and starburst galaxies?

OBSERVATIONS AND DATA REDUCTION

The data used in this project were collected on Kitt Peak, near Tucson, Arizona on the 2.1m Goldcam Spectrograph, and made available to use through funding provided by NOAO, NSF, and AURA.

First, AGN data was loaded into Graphical Analysis and probed for usable spectra. Each spectrum observed was placed into one of 4 categories: Elliptical galaxies, Radio galaxies, Starburst galaxies and Unusable Data. The last category was necessary because the data set contained other AGN not considered, such as blazers and quasars. In addition, a few of the files had breaks in the data in key areas of the spectrum, such that, their classification could not be determined. Once each file was categorized, the redshifts were calculated. The redshift equation can be stated simply as

$$1 + z = \frac{\lambda\ (obs)}{\lambda\ (rest)}$$

In the equation, Lambda is the wavelength, λ (obs) is the observed wavelength of a particular emission line, and λ (rest) is the rest wavelength of the identified emission line. The identity of each emission line used was found by calculating a ratio of two strong emission lines on each spectrum and referencing a table of ratios. (Rector, 2001) Once the redshift for each galaxy was calculated, an average redshift for each of the galaxy classifications was calculated, and the results were graphed using Microsoft Excel. It is also noted that due to the difficulty of separating radio and elliptical galaxies in our survey, these two categories were grouped together for further comparison.

ANALYSIS AND RESULTS

Elliptical and/or Radio Galaxy Redshifts
NGC 4742 = 3.005
NGC 6501 = 3.91
NGC 4589 = 1.7
NGC 5587 = 1.7
NGC 4486 = 1.7

Starburst Galaxy Redshifts
NGC 4395 = 0.71
M27 Center = 1.34
NGC 6058 = 1.31

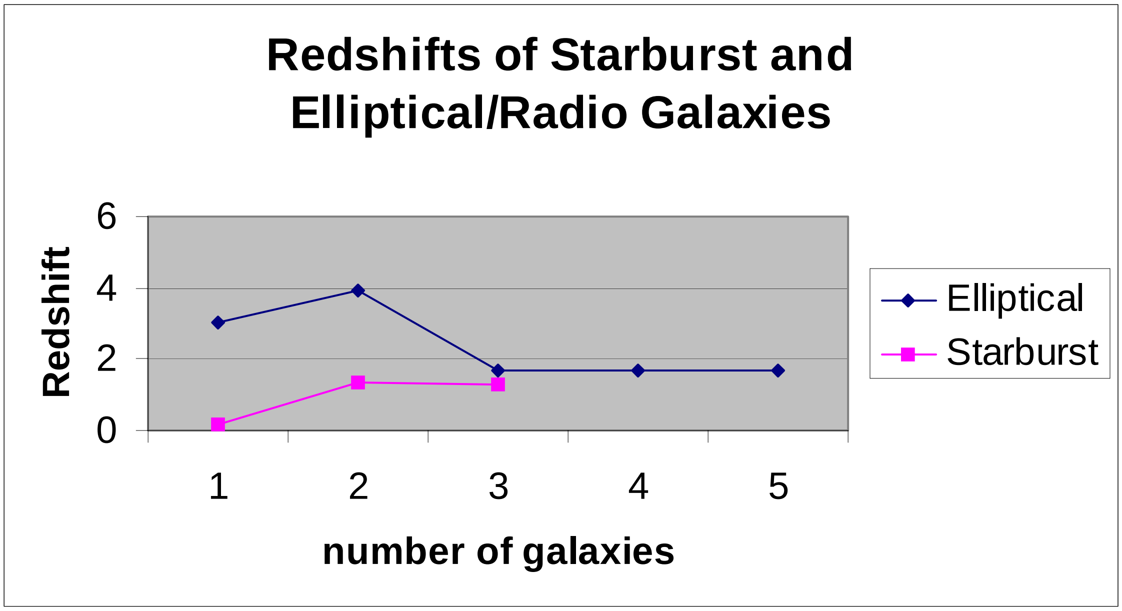

DISCUSSION

The results found with this research indicate that the redshifts of elliptical and/or radio galaxies are greater than that of starburst galaxies. There was no data to compare this study with because the project it was based upon, a previously unpublished study, was slightly different. This research shows a similar result, however, this research group disagreed with many of their classifications for the files in the data set. One of the problems encountered during our research was unusable data. Several files contained bad data points in the spectrum, were other types of AGN, or were found to be blueshifted. All of these were classified as unusable. These problems left us with a limited set of data. With the addition of data, these results could change.

SUMMARY AND ACKNOWLEDGEMENTS

All in all, the redshifts of elliptical/radio galaxies, as stated before, appear to be much greater than those of starburst galaxies. We would like to thank Mrs. Dowdy for making the data from NOAO (National Optical Astronomers Organization), NSF (National Science Foundation), AURA (Association of universities for research in astronomy) available to us. We would also like to thank Mrs. Tina Nance (Computer Technician) and Mr. Jim Whitaker (Math teacher) for providing the computers used to collect and analyze our data.

REFERENCES

Amazing Space, Website, *http://amazing-space.stci.edu/resources/explorations/galaxies- galore/teacher/scientific background.html*, January 7, 2005

Daily University Science News, *http://unisci.com/stories/20013/0907012.html*, January 7, 2005.

Dunbar, Brian, NASA Website, *www.nasa.gov*, January 7, 2005.
European Southern Observatory, Website, *http://www.eso.org/outreach/gallery/astro/*, January 6, 2005

National Optical Astronomy Observatory, Website, *http://www.noao.edu/image_gallery/elliptical_galaxies.html*, January 7, 2005

Radio Galaxy Information Guide, Website, *http://csep10.phys.utk.edu/astr162/lect/active/radio.html* (online journey through astronomy), January 7, 2005, Internet.

Rector, Travis A. and Wolpa, Brenda A., AGN Spectroscopy: Nature's Most Powerful Monsters" NOAO, October 1, 2001

Redshift Information Guide, Website, *http://www.astro.virginia.edu/~jh8h/glossary/redshift.htm* January 7, 2005

Stevens, Ian; Ponman, Trevor: Georgakakis, Antonis; Summers, Lesley Guerrero, Jimena Bravo; and Hartwell, Jo, Galaxies: Straburst Galaxies, Website, *http://www.sr.bham.ac.uk/research/starburst.html*, January7, 2005

Measuring the Microvariability of BL Lac

Tri Nguyen
Deer Valley High School, Antioch, CA
Teacher: Jeff Adkins, TLRBSE 2002

ABSTRACT

During the night of October 23, 2004, observations were taken by Tri Nguyen at Kitt Peak National Observatory to measure the microvariability of the Active Galactic Nucleus, BL Lac, the first blazer ever found. Using the images observed from the night of October 23, 2004, v-magnitude data was extracted and used to construct a light curve of this object. From this graph, greatest changes in variation of approximately 0.0393 magnitude occurred over several minutes. This shows that it is not significant compared to the measured error. This confirms that BL Lac had little changes in magnitude showing no significant variations on a time scale of minutes.

INTRODUCTION:

Active Galactic Nuclei (AGN) are galaxies that transmits high amounts of energy from their core and are believed that the galaxies core are black holes. These galaxies are surrounded by an accretion disk that is composed of debris, high-energy particles, and radiation. The black hole emits high levels of photons that are gamma rays and there are correlations between masses of these black holes and velocity dispersions in active galaxies. (Kotilainen, J., Falomo, R. & Treves, A. 2003) Around the accretion disk is a cloud shaped object of matter that blocks off some of the gamma rays called the torus. There is evidence that there are jets that shoot out gamma ray radiation. There are two beams of these jets each in opposite directions of the black hole. The interaction of these jets with galaxies has a relationship in the role for acceleration of high-energy particles in Active Galactic Nuclei (Pohl, M. 2003)

Because these Active Galaxies vary on different time scales, there are different phenomena at the core of active galaxies that can cause measurable variability on a time scale of minutes and hours. Over the past several years, there has been evidence variability for many types of Active Galactic Nuclei. (Miller, H. et al. 1999, Massaro, E., et al. 1999, Nesci, R. et al. 1999, Millar, H.R. et al. 1999, Tosti , G. et al. 1999, De Diego, J.A. et al. 1997) Microvariability in BL Lac been detected before on August 30, 1997, where there was a rapid and linear increase. The variation detected was about 0.50 magnitude in less than 90 minutes. (R. Speziali & G. Natali 1998) The purpose of this paper is to detect luminosity changes and provide data of the microvariability of the Active Galactic Nuclei, BL Lac.

OBSERVATIONS AND REDUCTION

Observations were taken using the Wisconsin Indiana Yale NOAO (WIYN) 0.9 meter telescope at Kitt Peak near Tucson, Arizona and the CCD camera used was S2KB (2048 x 2048 Silicon Imaging CCD Camera). The Unix computer called "Olive" controlled the telescope and the computer called "Taupe" controlled the camera. The computer, running the UNIX operating system, uses a program called IRAF (Image Reduction and Analysis

Facility), which is used on “Taupe” to perform the data reduction and data acquisitions. (Tody 1993) Data reduction is needed to reduce the raw image by subtracting all sources of noise and electron buildup given from the electronics. This is needed in order to get the highest quality image of the object being observed. There are three types of errors involved and can be corrected using Bias Frames, the readout differences for each pixel, Flat Frames, the optical imperfections in the telescope and camera, and Dark Frames, the electronic chip noise and temperature. Bias and Flat Frames were only needed for the data reduction. Dark Frame is not needed with this particular camera/telescope because the camera is chilled with liquid nitrogen.

On October 23, 2004, during the afternoon, preparations were made before observing by taking these types of frames. The bias frames were made using a 0 second exposure time. Approximately 10 exposures were made. Flat frames were made with each type of filter. Before they were taken, the Dewar was filled with liquid nitrogen to keep the electronics cool and was refilled every 8 hours. In the control room, the telescope was slewed to the mirror cover park position so that the cover could be taken off. After taken off, the telescope was slewed to the dome flat park position which points to a white flat circle in the dome. Five Flat Frames were made for each type of filter. The filters were B, V, R, and H-alpha. Each filter has its own Dome Flat Exposure Settings. For these four filters, the Lamp Setting is at low luminosity at 100%. The exposure times for these filters were: B–13sec, V– 5sec, R– 3s, H-alpha- 60sec.

After the bias and flat frames were taken, to begin observing, the dome shutter was opened and dome fans were turned on. Also, the dome vents were opened and dome lights were turned off. In the control room, we slewed the telescope to zenith. Then we moved the telescope to a bright star near the zenith and turn on telescope tracking and auto dome. To begin observing, we went to the first object and checked to make sure the telescope was in focus. Images were taken beginning at 6 PM.

At around 9PM, we started taking images of BL Lac using a V filter. Using the exposure time calculator from the NOAO website, we used an exposure time of 4 seconds for a 100 signal-to-noise ratio (SNR) at the given magnitude of 14.5 from the GTN Program Catalog. (Computing Exposure Times with the IRAF Task CCDTIME 2004) Unfortunately the brightness counts only showed up around 400 brightness counts (BC, pixel value). We raised the exposure times to 30 seconds and the BC were around 3500. Again, we raised the exposure to 60 seconds to get brightness counts of around 6000. This exposure time seemed to be the best maximum SNR without over exposing the image. With the signal to noise improved, we stayed on this object taking images until around 10:35PM. To make sure the objects were still in focus, we checked the various stars around the image using IRAF’s profile tool which graphs the pixel value (y-axis) and the Radius (x-axis).

Image Calibrations were made using IRAF after all observations were taken. The bias and flat frames were averaged and then subtracted from the raw image. Katy Garmany did these image calibrations.

DETERMINING MAGNITUDES

Using the calibrated images, the program, HOU Image Processing, was used to extract brightness counts off each image by using finder charts for the AGN and the standard stars given in the Global Telescope Network (GTN) program catalog.

Figure 1. Finder chart of BL Lac from GTN Program Catalog (Spear 2004). The letters represent names for the standard stars and BL Lac is located with the bracket lines.

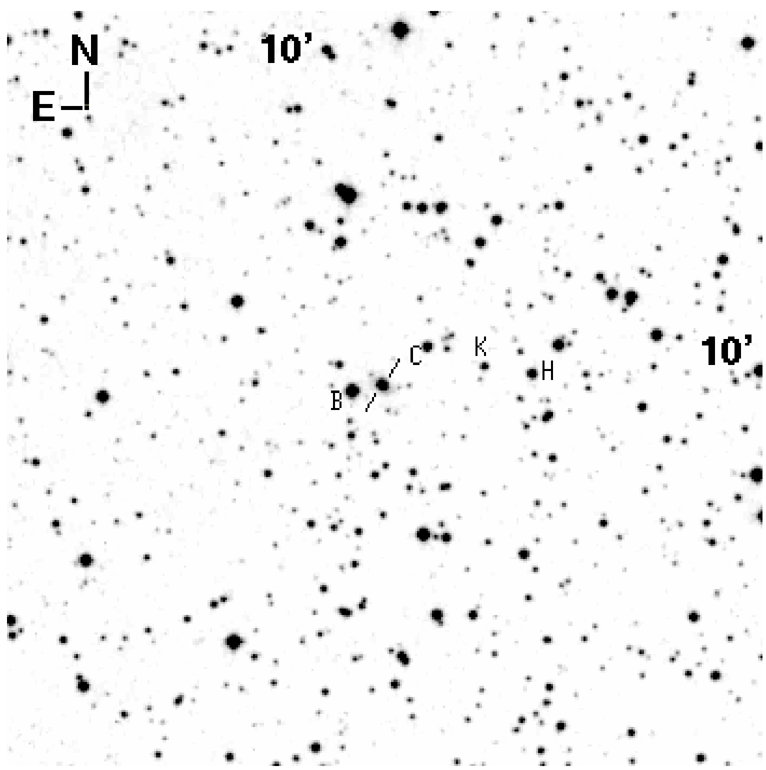

Table 1. List of standard star magnitudes for BL Lac for V filters from GTN Program Catalog (Spear 2004).

Star	V	V Uncert.
B	12.78	0.04
C	14.19	0.03
H	14.31	0.05
K	15.44	0.03

Figure 2. This is a sample images taken on October 23, 2004 at Kitt Peak National Observatory using the 0.9 meter WIYN telescope. (Image 10) The red circles are the apertures that are directed around the standard stars and BL Lac.

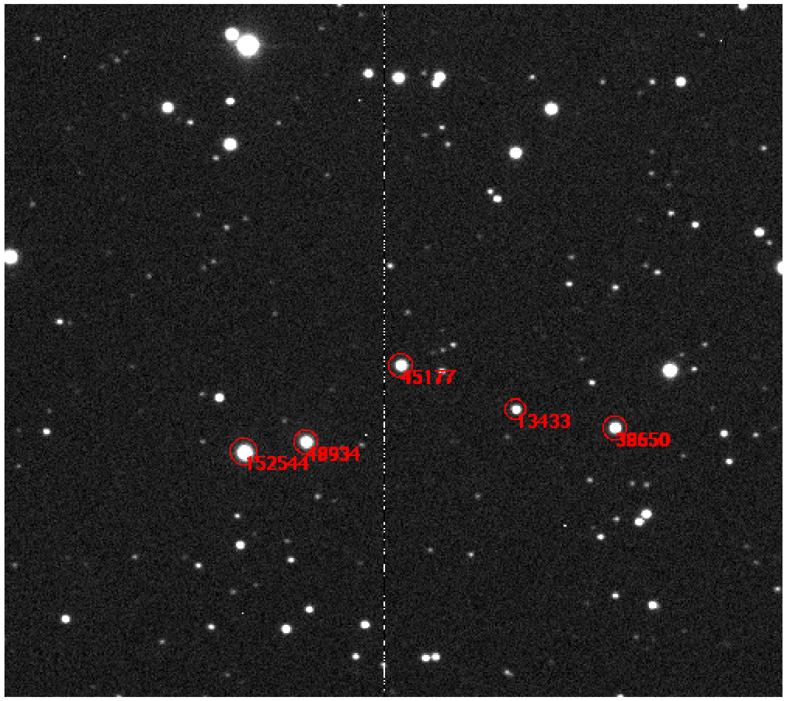

An aperture was directed around each object, the AGN and Standard stars, to obtain their brightness counts. The size of the aperture was set at the default, an auto-aperture, making the aperture size adjust to the size of the star. The auto aperture tool pre-calculated the radius and sky radius by finding a background sky value. This is completed by sampling pixels around an annulus of radius 25 pixels, which is centered at the local maximum in the area of the pixel selected by the mouse click. The sky value is assigned to be the median of the pixel values in the annulus.

In certain images, there was a bad row, which overlapped the standard star C, because of this problem, star C was omitted to correct the problem during the magnitude calculation, but only for those images that were overlapped. In figure 2, the bad row appears, but does not overlap standard star C.

The statistical analysis program, Fathom, was used to compute magnitudes. (Fathom c 2004) The data of brightness counts was input into a table including the magnitude of the standard stars given in the Global Telescope Network (GTN) catalog.

Table 2. Example of Magnitude and Brightness Counts of Standard Stars taken from Image 11

Collection 1

	star	MagnituÉ	BrightnÉ	logbright
=				log (Brightne
1	Star B	12.780	164483	5.21612
2	Star H	14.310	41418	4.61719
3	Star K	15.440	14825	4.17099
4	Star C	14.190	48201	4.68306

Once computed, the data was plotted on a graph using this magnitude equation:

Equation 1:

$$M_1 = M_2 + 2.5 \log (B_2/B_1)$$

Figure 3. Example of Graph of Standard Star magnitudes vs. Measured Log of Brightness Counts from image 11

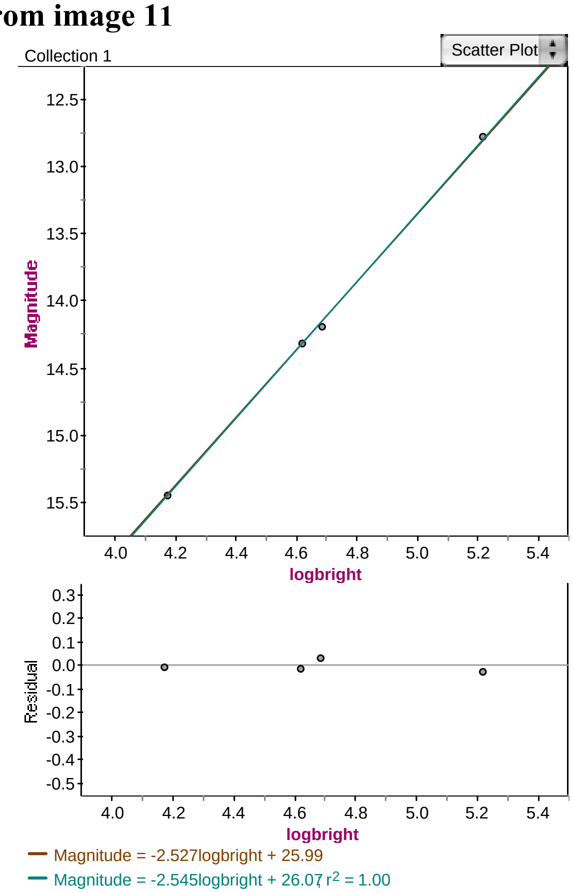

Using the Fathom program, a statistical analysis was made by making a simple regression model. It was calculated from the data set using the log of the brightness counts from the standard stars and BL Lac and the standard stars magnitudes to get the magnitude and error of the AGN, BL Lac. In order to build a simple regression model, the response attribute, Magnitude, and a predictor attribute, logbright, had to be selected by dragging the Magnitude and logbright from the graph to the model window. Once the simple regression was formed, it gave a computed magnitude of BL Lac with error. The error was calculated using a one sigma confidence level.

Figure 4. Example of Simple Regression of Magnitude and the log of brightness from image 11

BL Lac BC = 53286
Log of BL Lac = 4.72661

Model of Collection 1 — Simple Regression

Response attribute (numeric): Magnitude
Predictor attribute (numeric): logbright

Sample count: **4**

Equation of least-squares regression line:
Magnitude = **-2.54462 logbright + 26.068**
Correlation coefficient, r = **-0.999719**
r-squared = **0.99944** , indicating that **99.944** % of the variation in **Magnitude** is accounted for by **logbright** .

The best estimate for the slope is **-2.54462** +/- **0.0544421** at a 67 % confidence level. (The standard error of the slope is **0.042654** .)

When **logbright** = 4.72661 , the predicted value for a future observation of **Magnitude** is **14.0406** +/- **0.0452476** .

The Universal Time from each image was converted to a Julian Date using a Julian Date converter. (Julian Date Converter 2004) Then all magnitude, error, and Julian Dates from the BL Lac Images were put into a table to construct a light curve. After all data was collected, a light curve for the object, BL Lac was made.

A light curve for Standard star C was also made to confirm the technique in converting brightness counts to magnitude was correct. This technique is valid because the light curve of standard star C is flat with no variations as shown in figure 5.

Figure 5. Light Curve of Standard Star C.

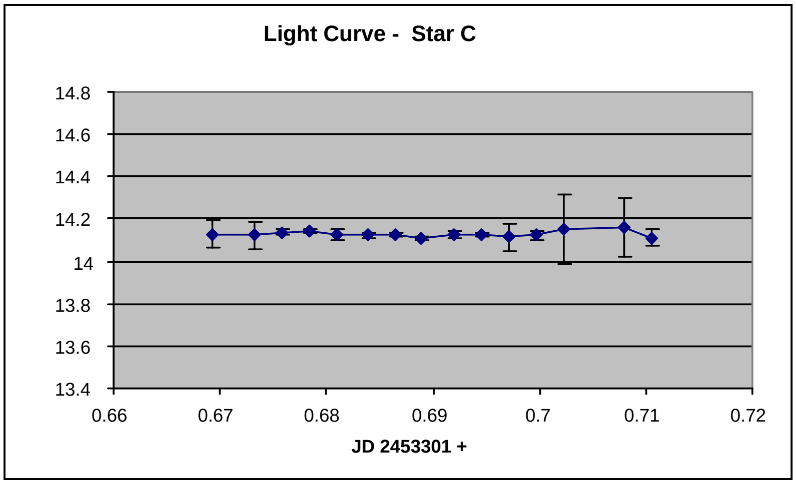

Table 3. The table below represents the slopes and y-intercepts from the line of best fit used to calculate magnitude for each individual image.

Image Number	Slope of Standard Star Fit	Intercept
1	-2.53106	26.05
2	-2.51503	25.892
3	-2.53133	25.994
4	-2.53123	25.948
5	-2.54173	26.06
6	-2.53938	26.059
7	-2.5449	26.054
8	-2.52314	25.927
9	-2.50866	25.962
10	-2.50918	25.822
11	-2.54462	26.068
12	-2.53688	26.018
13	-2.56133	26.156
14	-2.54243	26.037
15	-2.5385	26.015
16	-2.53558	26.029
17	-2.54834	26.091
18	-2.54124	25.688
19	-2.49922	25.388
20	-2.54339	25.892
21	-2.52084	25.973
22	-2.57016	26.226
23	-2.51572	25.942

Table 4. All computed magnitudes, Julian dates, errors, and exposure times for BL Lac

Image Number	Magnitude	Error	Min	Max	JD2453301+	Exposure Times (seconds)
1	14.0472	0.03402200	14.01317800	14.08122200	0.66926	60
2	14.0503	0.01836480	14.03193520	14.06866480	0.67324	60
3	14.0406	0.02721820	14.01338180	14.06781820	0.67579	60
4	14.0215	0.02387140	13.99762860	14.04537140	0.67834	60
5	14.0469	0.02062670	14.02627330	14.06752670	0.68089	60
6	14.0357	0.01005800	14.02564200	14.04575800	0.68384	60
7	14.0419	0.00442795	14.03747205	14.04632795	0.68639	60
8	14.0298	0.02959860	14.00020140	14.05939860	0.68895	60
9	14.0447	0.06191340	13.98278660	14.10661340	0.69203	60
10	14.0339	0.06695120	13.96694880	14.10085120	0.69457	60
11	14.0406	0.04524760	13.99535240	14.08584760	0.69714	60
12	14.0332	0.04231180	13.99088820	14.07551180	0.69970	60
13	14.0469	0.05805040	13.98884960	14.10495040	0.70225	60
14	14.0418	0.05993730	13.98186270	14.10173730	0.70802	60
15	14.0247	0.05982310	13.96487690	14.08452310	0.71057	60
16	14.0315	0.07013180	13.96136820	14.10163180	0.71312	60
17	14.0332	0.05753380	13.97566620	14.09073380	0.71568	60
18	14.0319	0.05705070	13.97484930	14.08895070	0.71896	60
19	14.0282	0.07305960	13.95514040	14.10125960	0.72150	60
20	14.0334	0.06119840	13.97220160	14.09459840	0.72448	60
21	14.0440	0.08813750	13.95586250	14.13213750	0.72703	60
22	14.0608	0.07507070	13.98572930	14.13587070	0.72958	60
23	14.0308	0.07253380	13.95826620	14.10333380	0.73214	60

This object was monitored only for one night due to cloudiness, humidity, and turbulence, but with the data collected, it showed very little direction toward microvariability. The results of the variation detected are displayed in figure 6 and table 4. Greatest changes in variation of approximately 0.0393 mag occurred over several minutes. This is not significant compared to the measurement error.

CONCLUSIONS

The observations revealed that there were no large variations in brightness on timescales of minutes that were observed for the Active Galactic Nuclei, BL Lac on the night of October 23, 2004. Though there were no variations found in this night, BL Lac has had variations detected from it before. Microvariability of active galaxies are uncommon, but are likely to be seen. There has been no pattern of microvariability occurrences. Variations from active galaxies are often wild making them unpredictable and rare to be seen, but searching for these types of variations when found can help find out more information on active galaxies because there is little information in this area. Although there were no significant variations found on this night, continued research will be conducted to find these types of variations. If these variations are found, it can be used to find the size of the event horizon of the black hole in light-minutes or light-hours.

Figure 6. The light curve for BL Lac obtained on October 23, 2004.

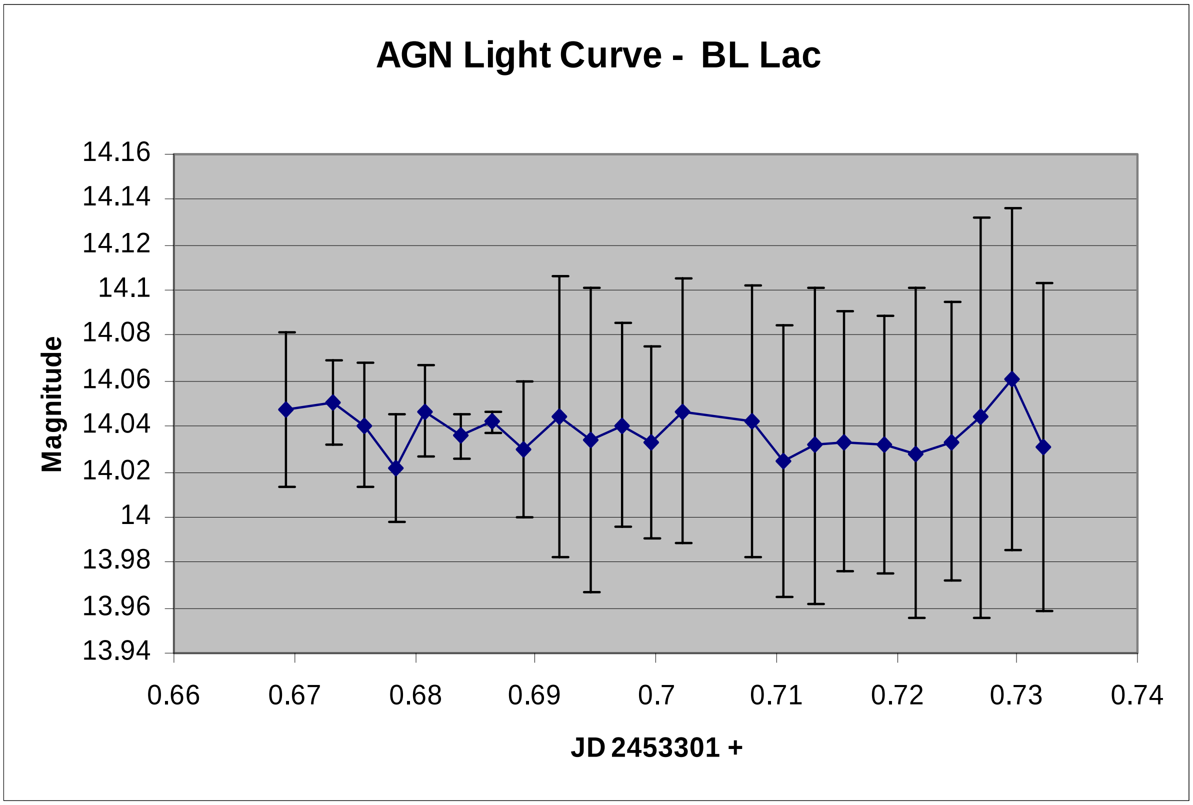

ACKNOWLEDGEMENTS

Special thanks to Teacher Leaders in Research Based Science Education (TLRBSE), Kitt Peak National Observatory (KPNO), National Optical Astronomy Observatory (NOAO), Global Telescope Network (GTN), and the Deer Valley High School ESPACE Academy.

REFERENCES

Computing Exposure Times with the IRAF Task CCDTIME. 16 Mar. 2004.

National Optical Astronomy Observatory (NOAO). 17 Oct. 2004 <*http://gtn.sonoma.edu/public/resources/active_galaxies/*>.

De Diego, J.A. et al.: 1997, Astronomy and Astrophysics. 318, 331-336

Fathom, Statistical Analysis Software: version c.: Key Curriculum P, 2004.

Julian Date Converter. 14 July 2004. U.S. Naval Observatory. 27 Oct. 2004 <*http://aa.usno.navy.mil/data/docs/JulianDate.html*>.

Kotilainen, J., Falomo, R. & Treves, A.: 2003, ASP Conference Series, Vol. 299, p.77-82

Massaro, E. et al.: 1999, ASP Conference Series, Vol. 159, p.79-82

Miller, H. et al.: 1999, ASP Conference Series, Vol. 159, p.75-78

Millar, H.R. et al.: 1999, ASP Conference Series, Vol. 159, p.143-144

Nesci, R et al.: 1999, ASP Conference Series, Vol. 159, p.141-142

Pohl, M.: 2003, ASP Conference Series, Vol. 299, p133-142

R. Speziali & G. Natali. ArXiv: astro-ph/9809109 v1 9 Sept 1998

Spear, Gordon. Global Telescope Network Program Object Catalog. National Aeronautics and Space Administration (NASA). 6 Oct. 2004 <*http://gtn.sonoma.edu/participants/catalog/index.php*>.

Spear, Gordon. Global Telescope Network Active Galaxies. National Aeronautics and Space Administration (NASA). 6 Oct. 2004 <*http://gtn.sonoma.edu/public/resources/active_galaxies/*>.

Tody, D. 1993, "IRAF in the Nineties" in Astronomical Data Analysis Software and

Systems II, A.S.P. Conference Ser., Vol 52, eds. R.J. Hanisch, R.J.V. Brissenden, & J. Barnes, 173.

Tosti, G et al.: 1999, ASP Conference Series, Vol. 159, p.145-148

RV Tauri Stars: Spectral Rebels

Nathan J. Stano, Graham T. Kozak, and Zackery J. Schroeder
Grosse Pointe North High School, Grosse Pointe Woods, MI
Teacher: Ardis Maciolek, RBSE 1998, TLRBSE 2001

ABSTRACT
The intent of the project was to gain insight into the possible mechanisms that explain the peculiar chemistries and changes in RV Tauri stars, and to better understand where they fit in the stellar evolution sequence. Spectral analysis was cross-correlating with the changes in the light curves of RV Tauri stars. RV Tauri stars were also compared with model stars using the Vienna Atomic Line Database and with similar stars from the Paranal Observatory catalogue. The major discovery was that the metallicities of the RV Tauri stars increased as they drew toward their light curve minima. This may be due to dredging or breakout reactions that push heavier elements outward.

INTRODUCTION

RV Tauri stars are semi-regular pulsating variable stars. Their light curves are categorized by alternating deep and shallow minima as they change in size, their spectral type, and other changes. These stars have not been well studied since their discovery in the early 1900s. By studying these stars, a better understanding of where they fit in the progression of stellar evolution and why they behave so peculiarly can be achieved.

The intent of the project was to gain insight into the possible mechanisms that explain the peculiar chemistries and changes in RV Tauri stars, and to better understand where they fit in the stellar evolution sequence.

A literature search was conducted about RV Tauri stars to develop a profile of what is already known about their characteristics. It was found that their spectral type usually range from F and G at maximum, to G and early K at minimum, have a period ranging from 30-150 days between similar minima, and usually have a brightness range during this period of up to four magnitudes. On the HR Diagram, they are found above the horizontal branch on the high temperature side of the asymptotic giant branch. According to Light Curves of Variable Stars[1], RV Tauri stars are usually found in low metallicity globular clusters, where they are some of the most luminous stars in those clusters, but most of the RV Tauri stars are found as field stars, where they aren't necessarily low metallicity. In addition to this, there are two types of RV Tauri stars, a and b. RVa's, such as R Scuti, have a relatively constant brightness in their variability, while RVb's, like RV Tau, have long term periodicity. Also, RV Tauri stars are related to other variable stars, specifically Type II Cepheids, W Virginis stars, BL Hercules, and UU Hercules stars. The similarities are based on their location in low metallicity clusters, and other chemical similarities.

[1] Jaschek, C., & Jaschek, M. 1990, Cambridge, Cambridge Univ. Press

OBSERVATIONS AND DATA REDUCTION

The first task was to sort through spectra of 11 variable stars obtained at the Coude Feed Spectrograph. Using the AAVSO Light Curve Generator, light curves for the RV Tauri stars were calculated, printed and plotted. Each date of observation was recorded as a point on the light curve so that the changes in the star's chemistry could be studied.

Using SIMBAD, spectra obtained from Kitt Peak National Observatory were identified as from RV Tauri stars. SIMBAD was also used to find the published spectral types of the stars. Spectra were then analyzed using Graphical Analysis 3.0, to measure line depths and equivalent widths to calculate the abundances.

Certain elements were chosen for analysis. These elements include carbon, hydrogen, titanium oxide, and calcium. These chemicals and wavelengths were chosen based on the recommendations from The Classification of Stars[2]. The ratio of Fe/H was calculated as a standard for the comparison of metallicity. The other ratios were calculated to help determine amounts of elements such as carbon and titanium, which are known to fluctuate in these stars and to refine their spectral class. The ratios Fe/H, CH/Fe, Ca/H, CN/Fe TiO/Fe were calculated.

The European Southern Observatory's UVES Paranal Observatory Project was used to find a group of stars with similar chemistry to RV Tauri stars. Stars were chosen based on spectral type, variability, and quality of spectra. Vizie-R was used to obtain data on them, such as the absolute magnitude, mass, period, and range. The equivalent widths and abundance ratios for these stars were calculated using the same standards as the RV Tauri stars.

For the similar variable stars, the same ratios were used as on the RV Tauri stars to compare and contrast the metallicity and formulate a hypothesis on why these RV Tauri stars do not behave like the other variable stars.

Using the Vienna Atomic Line Database (VALD), model stars were created to compare to the RV Tauri stars. These model stars represent what chemistries the RV Tauri stars should contain if they were not irregular. To use the VALD, data on the star's microturbulence, log of gravity, effective temperature, and wavelength ranges. If these factors could not be found by database searches, they were estimated. This technique gives a better idea of how these stars deviate from stars that would be of the same spectral class, and other factors of the RV Tauris.

Using the Jacoby Atlas, standard stars were found and analyzed. These stars are examples of what a star of a certain spectral class should look like without any

[2] Jaschek, C., & Jaschek, M. 1990, Cambridge, Cambridge Univ. Press

abnormalities. These stars were used to identify some of the spectral classes of the other stars, as well as the RV Tauri stars as they changed during different observations.

ANALYISIS AND RESULTS

The row headings in the analysis table state the star's name, its type, and calculated ratios of equivalent widths of lines. N/A was used when data was not available. Next, the published spectral type was compared with the observed spectral type of the star,its period and magnitude range.

The sample light curve shows and example of how different dates were plotted to see what state the RV Tauri star was in when it was being observed (for instance, near a maximum or a minimum of light).

Analysis Ratios and Properties of Selected Stars

Star Type	Fe/H	CH/Fe	CN/Fe	TiO/Fe	Published	Observed		
RV Tauri	4045/4101	4295/4325	4216/4045	4584/4250	Spectral Type	Spectral Type	Mag. Range	Period (days)
V453 Oph	0.59	0.77	1.36	N/A		F8Ib	13.4- 14.0	2.85
AC Her	1.67/1.08/.67/.55	.47/1.37/.95	1.33/.69/.43/.42	N/A	F4Ibpvar	G3I, G4I, G5I, F4I	6.85- 9.0	75.01
TT Oph	.6/.63	.342/.625	0.6/.54	N/A	F5pe	K5I	9.5- 10.8	61.08
V360 Cyg	8.00	0.40	0.75	N/A	F8	G1I	10.36- 12.23	70.39
TX Oph	4.74/.89/.95/.88/1	1.5/.94/1.11/4.74	5.63/1.13/.88/.69	N/A	G0	G1I, G3I, K5I	9.7- 11.4	135.00
R Sge	1.33/1/1.13	.71/.2	1.5/.94	N/A	G0Ib	G3I, K5I	8.0- 10.4	70.77
UZ Oph	1.13	9/.70/	1.25/.79/1	N/A	G2	K5I	9.9- 11.5	87.44
AD Aql	.63/1.538	2.5/.67/.91	1.08/.25	N/A	G8	F4I, F0III	11.5- 13.5	65.40
V Vul	1.9/3.809	.5/4.5/5.83	1/.842	N/A	G8Iab:var	G1I, K5I	8.1- 9.5	75.70
R Sct	N/A	N/A	1.63/.75/1.54/1.8	1/2	K0Ipbvar	K2III, G0I, G2I,	4.5- 8.6	146.50
V564 Oph	N/A	N/A	1.87	0.80	K2	K5I	9.4- 10.9	70.33
Paranal						Star Type		
HD 154365	0.22	0.95	N/A	N/A	G0II	Delta Cep	6.6- 7.3	6.64
HD 2151	1.09	0.44	1.50	N/A	G2IV	Variable	6.9- 7.7	4.07
HD 92626	5.83	2.50	2.00	N/A	G8/K0p	Carbon	2.75- 2.81	
HD 206778	N/A	N/A	0.36	1.33	K2Ib	Variable	0.7- 3	
HD 159532	0.94	N/A	N/A	N/A	F1II	Variable		
HD 27290	2.67	N/A	1.00	N/A	F4III	Pec. Var.		
HD 54605	0.50	0.67	N/A	N/A	F8Iab	Variable		
VALD								
V453 Oph	1.05	N/A	N/A	N/A				
AC Her	3.56	N/A	N/A	N/A				
TT Oph	0.91	N/A	N/A	N/A				
V360 Cyg	0.01	N/A	N/A	N/A				
TX Oph	0.54	N/A	N/A	N/A				
R Sge	0.54	N/A	N/A	N/A				
UZ Oph	0.13	N/A	N/A	N/A				
AD Aql	0.67	N/A	N/A	N/A				
V Vul	0.67	N/A	N/A	N/A				
R Sct	0.67	N/A	N/A	N/A				
V564 Oph	0.67	N/A	N/A	N/A				

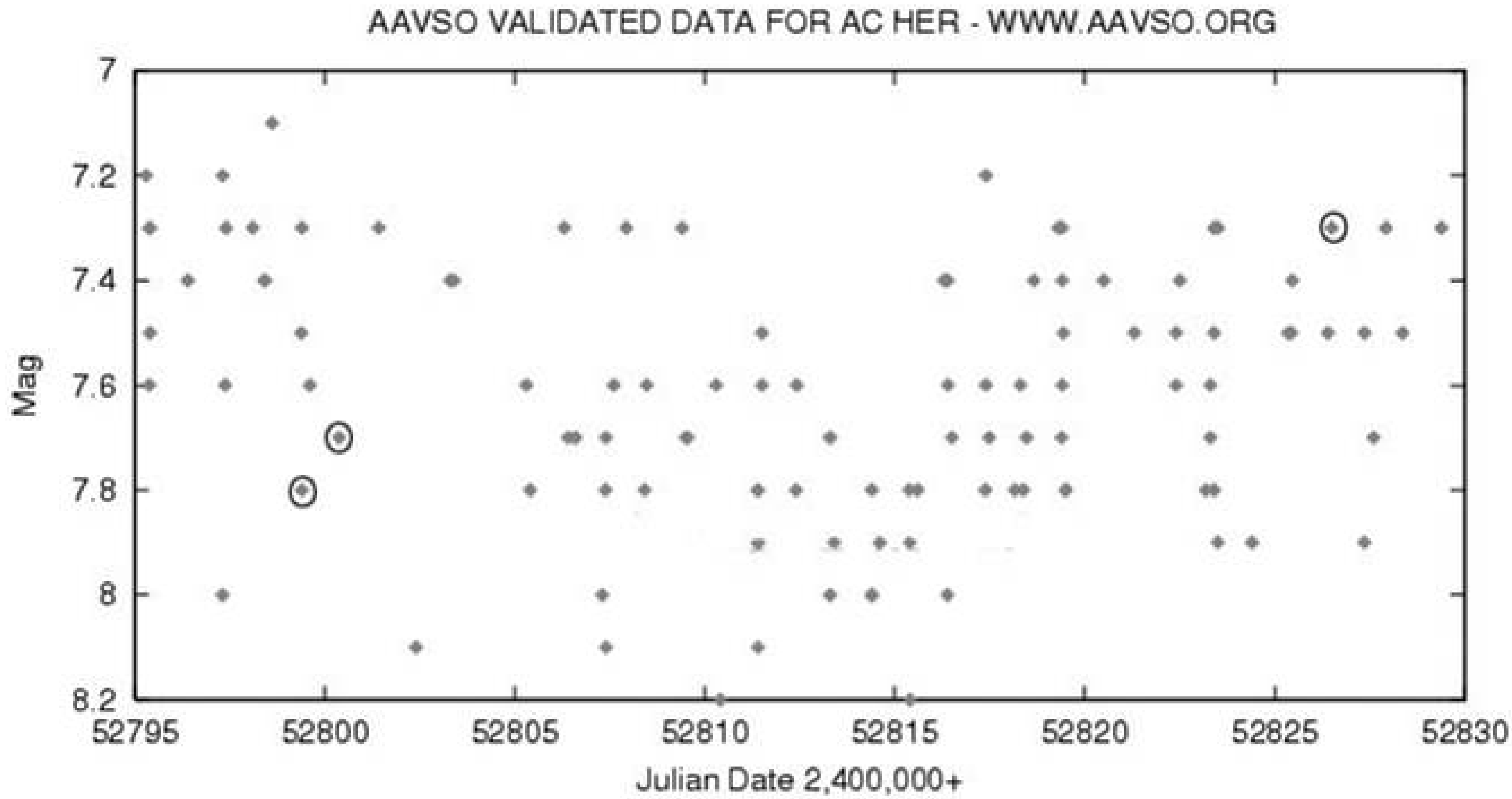

Circled points represent dates of observed spectra.

DISCUSSION

Upon analysis, the RV Tauri stars do show chemical abundances that change over time. These changes tended to vary from star to star. Some stars were oxygen rich, while others were carbon rich. Those that were oxygen rich tended to have the strong titanium oxide lines.

It was observed that as the stars approached minima, their metallicities increased as compared to at maximum. When the RV Tauri stars were compared to the VALD models, no pattern in metalliticites could be found. When the RV Tauri stars were compared to the Paranal stars, again no pattern could be found.

In the star UZ Ophiucus, emission lines were observed in one of the hydrogen lines. It was concluded that the hydrogen near the surface was pushed outward and formed a cloud that was heated to the point of it producing its own light on the hydrogen wavelength, interfering with the spectrum of the star.

One possible explanation for the odd abundances in RV Tauri stars is dredging. What happens is that elements that were being used in the star's nuclear reactions are, for some reason, brought to the surface. This explains the amounts of carbon, oxygen, and titanium oxide.

Upon research, it was found that in some hot stars a "breakout" reaction could occur. This reaction is a runaway nuclear reaction, which is usually very short, only 10-1000 seconds, which can result in the fast creation of denser elements, like titanium. This may also explain the fast, shallow interruptions in the somewhat normal cycle of the deeper minima.

The appearance of carbon and oxygen in such ample supply could be due to breakouts. As these happen, the elements produced are pushed outward toward the stellar atmosphere, where they can be observed as the star expands. When both the carbon or oxygen and other created elements have been pushed out, the star shrinks, and the process continues again.

SUMMARY AND ACKNOWLEDGEMENTS

In short, it has been concluded that the peculiar metallicities of RV Tauri stars may be due convective dredging and to "breakout" reactions. Oxygen and titanium abundances appear to fluctuate in direct proportion to each other. Changes in metallicity correlate with the star's light curve. As the light decreases, the metallicity increases.

REFERENCES

American Association of Variable Star Observers . American Association of Variable Star Observers. 26 Mar. 2005 <*http://www.aavso.org/*>.

Bagnulo, S, et al. "The UVES Paranal Observatory Project ." ESO/Chile Facilities in Santiago. 17 Feb. 2005. European Southern Observatory. 26 Mar. 2005 <*http://www.sc.eso.org/santiago/uvespop/*>.

Jaschek, Carlos, and Mercedes Jaschek. The Classification of Stars. 1987. Cambridge, England: Cambridge University Press, 1990.

Jaschek, Carlos, and C Sterken. The Light Curves of Variable Stars. Cambridge, England: Cambridge University Press, 1996.

SIMBAD Astronomical Database. Centre de Données Astronomiques de Strasbourg . 26 Mar. 2005 <*http://simbad.u-strasbg.fr/Simbad*>.

VizieR. Centre de Données Astronomiques de Strasbourg . 26 Mar. 2005 <*http://vizier.u-strasbg.fr/viz-bin/VizieR*>.

Multiple Periodicities of RV- Tauri Variable Stars

Glenn Ferreira
Westford Academy, Westford, MA
Teacher: Joan Kadaras, TLRBSE 2003

ABSTRACT
I studied the periodicities and associated factors of the RV Tauri variable star, Epsilon Lyra. Because the apparent magnitude light curve on AAVSO does not follow a clear or coherent periodicity, I am testing whether the luminosity is governed by multiple properties (mainly radius, and temperature because of the L=4*pi*σ*t^4*r^2 formula), which hypothetically have independent differing periodicities. The magnitude/periodicity would be a composite of these separate properties. I determined short and long term periods for the stars, based off light curves and varying recession velocity.

INTRODUCTION

RV Tauri variable stars fall on a particular region of the Hertzsprung-Russell Diagram (note particular location on chart). This diagram has absolute visual magnitude (in effect brightness) on the y-axis and spectral class (in effect temperature) on the x-axis. A star location on this chart, as well as its "behavior" categorizes it as a particular type of star (RV Tauri, Semi-regular, Cepheid etc). The "behavior" of RV Tauri is best define by The General Catalogue of Variable Stars (Kholopov 1985), which defines a RV Tauri Stars as --

> "pulsating supergiants having spectral types F to G at maximum light and K to M at minimum light. The light curves are characterized by the presence of double waves with alternating primary (deep) and secondary (shallow) minima which can vary in depth so that primary minima may become secondary ones and vice versa; the complete light amplitude may reach 3m to 4m in V. The periods between two adjacent primary minima (called "double" or "formal" periods) lie in the range 30 to 150 days. Two subtypes may be isolated: RVa- variables of RV Tauri type which do not vary in mean magnitude; RVb- variables of RV Tauri type which periodically vary in mean magnitude with periods of 600 to 1500 days, and amplitude up to 2m in V".

PROBLEM

When referencing the AAVSO light curves for RV Tauri stars, there is no obvious or coherent pattern. These charts plot the magnitude (easily converted to luminosity) over time. Luminosity/magnitude is governed by the equation,

Luminosity= 4*σ*pi*radius^2*temperature^4.

The four, pi, and Stefan-Boltzmann constant remain constant so they do not cause any variability in a star's brightness. So the temperature and/or radius must be changing in order for the luminosity and magnitude to change. Because the AAVSO light curves appear erratic, it is likely that both temperature and radius are changing [in a periodic manner] independent of one another. This can be conceptually proven by graphing two (or more) repeating continuous functions (i.e. sine or cosine) each with a periodicity (one to the second power to mimic radius, and one to the fourth power to mimic temperature). A seemingly erratic curve will be generated by plotting this over time. See U Mon chart, and the theoretical light curve chart for examples.

HYPOTHESIS

A- The luminosity/magnitude of RV Tauri stars is determined by two fluctuating factors varying with different periodicities in sinusoidal fashion. B- These fluctuating factors are the star's radius, and luminosity.

PROCEDURE -- for examining spectra without apparent magnitude or parallax:

1. Determine the spectral class (and luminosity class, if not available in simbad database) thru visual comparison to Jacoby's Atlas
2. Determine the spectroscopic parallax using a reference table
3. Convert the Absolute magnitude into Luminosity (Watts or Ergs), by creating a ratio Abs mag to luminosity for a known star (the sun) to your known star, Mstar – Msun = -2.5 log [Lstar / Lsun]
4. Determine the surface temperature (given by chart using spectral and luminosity class)
5. Convert the Absolute magnitude into Luminosity (Watts or Ergs), by creating a ratio Abs mag to luminosity for a known star (the sun) to your known star, Mstar – Msun = -2.5 log [Lstar / Lsun]
6. Determine the radius of the star Luminosity=4*pi* σ*Temperature(k)^4)*Radius^2, (Radius=(Luminosity/(4*pi*σ*Temperature(k)^4)^(1/2)
7. Identify several spectral lines
8. Determine the redshift of each line
9. Calculate the mean recession speed of the star

ANALYSIS AND RESULTS—

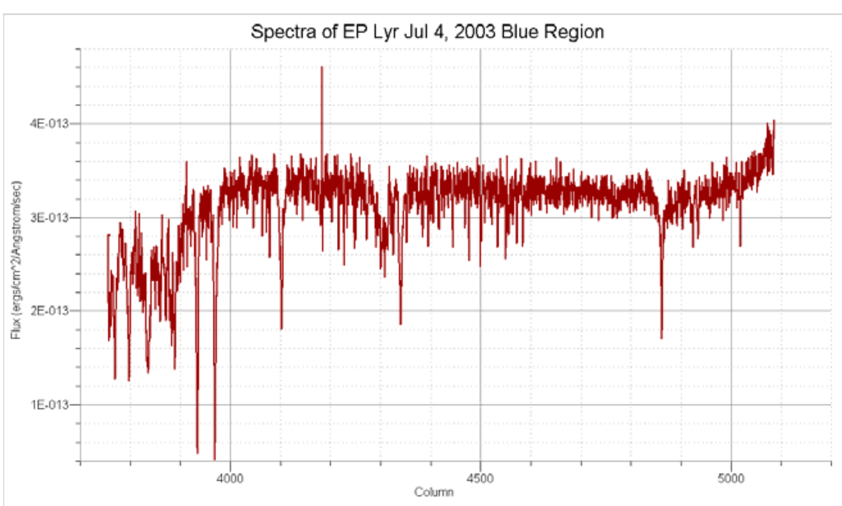

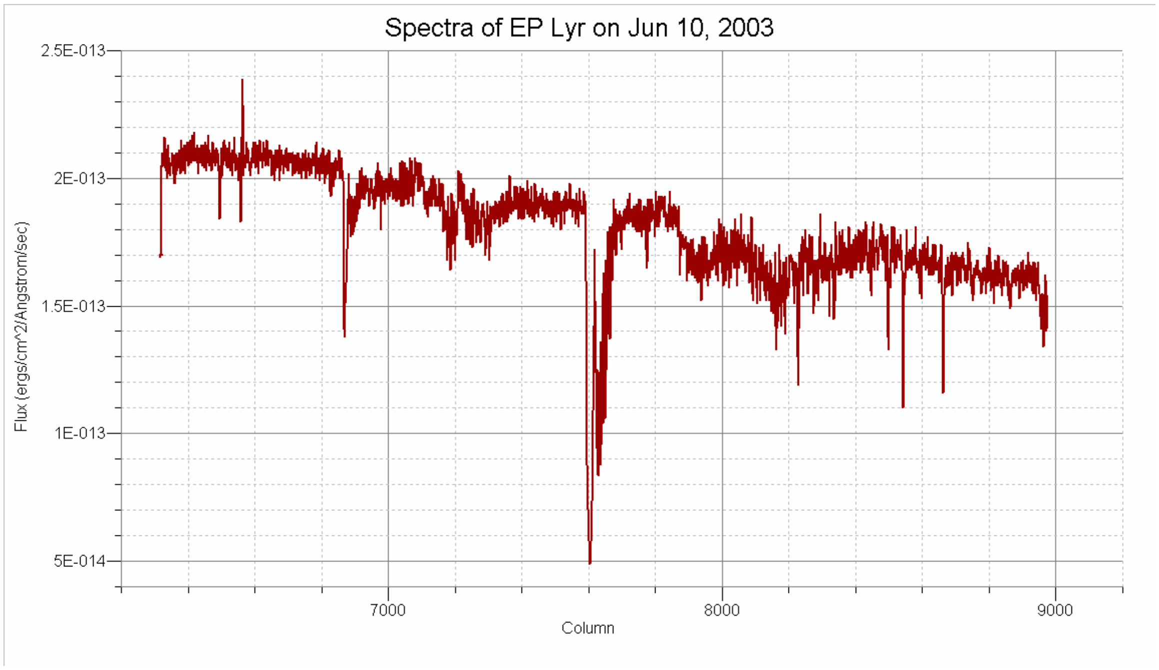

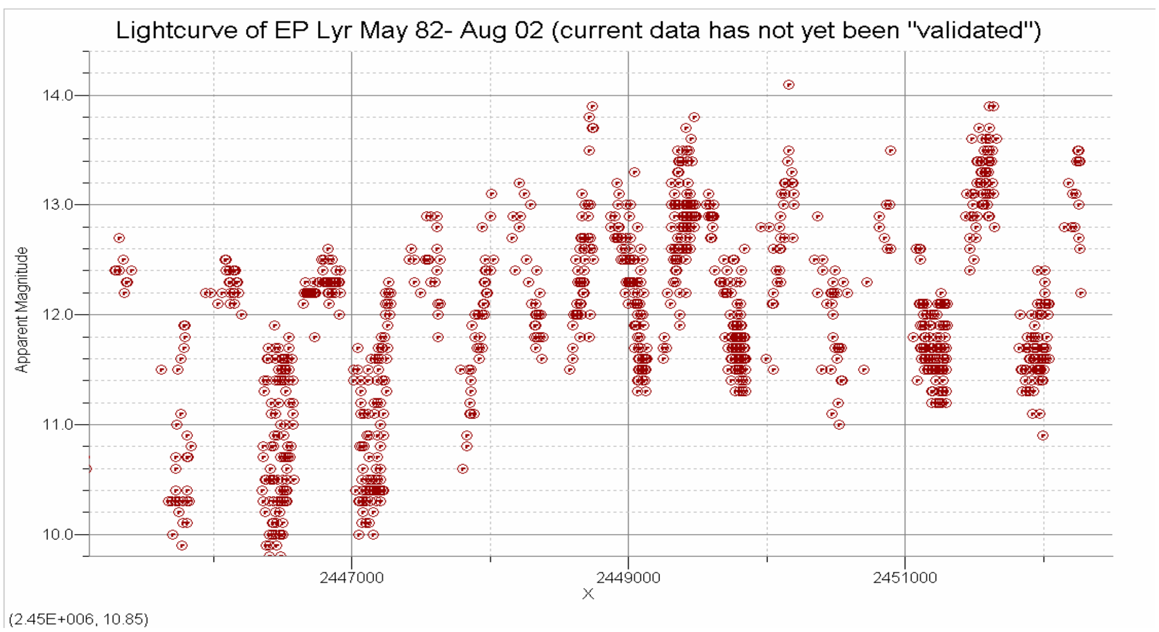

The long-term lightcurve has an easy-to-see pattern, which are sinusoidal in nature. These long variations are characteristic of RVb type RV Tauri stars, which have secondary periods of 600-1500 days. There are several distinct periods on the long term lightcurve. For the sake accuracy, the maximum around oct 84 is selected as the starting point, and April 94 the end point.

Start point-2446085.5
End Point- 2449445
5 cycles
(2449445-2446085.5)/5=671.9 days
The long term period of EP Lyr is ~672 days

Data (observed and calculated)

Date (stardard)		10-Jun-03		4.5-Jul-03
Julian		2452801.439		2452826.44
Spectral Type	G4 Ib		G3 Ib	
Abs Mag		-4.6		-4.55
Luminosity (Watts)		2.25E+30		2.15E+30
Temp K		5017		5083
Radius (M)		7.07E+10		6.73E+10

Radius Data

X	Y
2452801.439	70700000000
2452826.44	67300000000

Because of a scarcity of data, exact values for a sinusoidal pattern can not be found, but an approximant value can be determined

Y=A*SIN(B*X+C)+D	Very Approximant values (more accurately pictured as a range)	
A-amplitude	2.32E+11	+/- 1.82 E7
B-frequency	0.000628	+/- 1.17E-10
C- Phase	1	+/- .000294
D- offset	-1.58E+10	+/- 5.01E7
Max possible A(Frequency) -	0.000628	
Min Period	**10005 days**	

Temperature Data

X	Y
2452801.439	5017
2452826.44	5083

Because of a scarcity of data, exact values for a sinusoidal pattern can not be found, but an approximant value can be determined

Y=A*SIN(B*X+C)+D	Very Approximant values (more accurately pictured as a range)	
A-amplitude	-4.51E+03	+/- 3.01E6
B-frequency	0.000628	+/- .00171
C- Phase	1	+/- 1.42E4
D- offset	6.70E+03	+/- 7.79E6
Max possible A(Frequency) -	0.002338	
Min Period	**2687.4 days**	

Redshift Data

7/4.5/2003	**2452826.44**			
Line	**Observed (ang)**	**Theoretical (ang)**	**Redshift (ang)**	**Recession Speed (Km/s)**
H10	3797.3	3797	0.3	23.68712
Ca II K	3934.223	3933.68	0.543	41.384
Ca II H	3969.3	3968.5	0.8	60.43593
H epsilon	4101.3	4101.75	-0.45	-32.8908
H gamma	4340.1	4340.48	-0.38	-26.2469
TiO	4584	4584	0	0
H beta	4862.15	4862.68	-0.53	-32.6762
He I	4924.1	4922	2.1	127.9114
He I	5018.6	5016	2.6	155.3987
			Average=	**35.22259**

10-Jun-03	**2452801.439**			
Line	**Observed (ang)**	**Theoretical (ang)**	**Redshift (ang)**	**Recession Speed (Km/s)**
Ca I	6495.84	6495	0.84	38.77321
Fe I	8228.75	8227	1.75	63.77173
Ca I triplet	8498.6	8498	0.6	21.16733
Ca I triplet	8542.8	8542.1	0.7	24.56773
Ca I triplet	8663	8662.1	0.9	31.14949
			Average=	**52.8644**

Recession speed of a star is absolutely constant, so any deviations, are caused by the expansion or contraction of the star

Because of a scarcity of data, exact values for a sinusoidal pattern can not be found, but an approximant value can be determined

Y=A*SIN(B*X+C)+D Very Approximant values (more accurately pictured as a range)

A-amplitude	9.00E+00	+/- 3.74E7
B-frequency	0.113	+/- 25.3
C- Phase	-2.63	+/- 5.07E7
D- offset	4.42E+01	+/- 4.46E7
possible A(Frequency) -	0.002338	
Possible Period	**55.6**	

This period is only a average of other possible periods, but it is in the range expected for a RV Tauri star

Therefore the short-term period of Ep Lyr is around 55.6 days

DISCUSSION

The longest period observable in the lightcurve was 672 days, which is much less time then both of these periods. So from the data collected so far, it appears neither temperature nor radius affects luminosity in the proposed sinusoidal fashion. The changes of luminosity could be the result of other factors varying at sinusoidal rates, but there are no other characteristics capable of being measured from afar that could contribute to luminosity.

When examining the long term light curve for Ep Lyr, there appears to be a very long period (on the order of 20-50 years. The period appears to reach a maxima around JD 2449000, decrease sinusoidally before and after this time. This maybe be attributed to a change in radius and temperature (more likely radius), but additional long term data is needed to determine this.

From the data available, short-term variations seem chaotic, but the short term period can be measured by determining the difference in recession speed of a star. The velocity of the center of mass of Ep Lyr compared to that of our sun are extremely constant. However, the recession speed appears to change over time. As a star expands and contracts, it changes. The deviation between recession speeds is caused by this change in size. By analyzing this data in the same way as temperature and radius, a set of possible sine waves are generated. The frequency factor of this set of waves is more realistic. The average possible frequency produces a period of about 56 days. This is likely the short-term period of EP Lyr.

SUMMARY AND ACKNOWLEDGEMENTS

Ep Lyr displayed two periods clearly. The long period is reasonably accurate; the short period, however, is merely a mean value of several possibilities. Recession velocity is an indication of the stars period, and not a factor contributing to it. The long term light curve also showed a slight sinuscoidal pattern with a period of over 20 years, but there is insufficient data to examine this possibility. A special thanks to Joan Kadaras and Steve Howell for assistance in observing and analyzing these spectra and light curves, and to TLBRSE, NOAO, and NSF for making my observation at Kitt Peak possible.

REFERENCES

AAVSO:American Association of Variable Star Observers. American Association of Variable Star Observers. <*http://www.aavso.org*>.

Allen's Astrophysical Quantities. Ed. Arthur N. Cox. Rensselaer NY: AIP P, Springer, 2000. 381-396.

Chaisson, , and McMillan. Astronomy Today. Upper Saddle River, New Jersey : Prentice-Hall, 2002.

Croft, Steve, and Steve Howell. Spectroscopy of Variable Stars:. N.p.: n.p., 2004.

SIMBAD Astronomical Database. Centre de Données astronomiques de Strasbourg. <*http://simbad.u-strasbg.fr/Simbad*>.

Determining the Stellar Qualities of Stars Within Eclipsing Binary Systems

Kimmerlee Johnson
Great Falls High School, Great Falls MT
Teacher: Beth Thomas, TLRBSE 2004

ABSTRACT
A binary star is a system that contains more than one star. Binary systems can be classified according to the approach astronomers take to identify them. One such category is the eclipsing binary system. This type of system contains two stars that periodically eclipse each other, which changes the amount of light we see. Eclipsing binaries can be deciphered by observing the eclipse of one star by another through a light curve. In this project, spectrographs of several eclipsing binary systems were obtained from the Coudé Feed Spectroscope located at the Kitt Peak National Observatory in Arizona. Through these spectrographs, stellar qualities such as spectral class, absolute magnitude, luminosity, radius, mass, and density can be calculated.

INTRODUCTION

Star's whose light output varies are known as variable stars. These stars are sub-divided into two categories: intrinsic and extrinsic. Intrinsic variable stars' light variation is caused by a physical change occurring in the star or system, while extrinsic stars' light output varies due to an eclipse of one star by another. Eclipsing binaries are a type of extrinsic variable star. The systems usually consist of one star small in size with a high luminosity and another which is larger than the first but is not as bright. Because the inclination of the orbit of these systems lies near the line-of-sight of the observer, the system appears as only a single point of light. One way to distinguish that these stars are part of an eclipsing binary is to obtain a light curve of the system. The light curve of these systems will reveal two minimums, or decreases in luminosity. The first decrease, known as the primary minimum, is the greater of the two. A primary minimum occurs when the light from the brighter stars is eclipsed by the dimmer star. After the dimmer star passes in front of the brighter star, the luminosity will return to its original value. Halfway around the orbit, the brighter star passes in front of the dimmer star, which causes another decrease in the light output. This decrease will appear on the light curve as a secondary minimum, but is not as great as the primary. These differences in the minimas only occur because the stars' luminosity and size are not equivalent. Depending on the system, the eclipse could last a day to years.

RESEARCH QUESTION

If spectrographs of eclipsing binary systems are obtained, can their stellar qualities be determined? In addition, can the velocities of the gases within the systems be calculated to analyze the eclipse of the system? Through the calculations, will an eclipse be verified?

PROCEDURE

Eight eclipsing binary systems (see Chart 1) were selected to study using the Coudé Feed Spectroscope. These systems were selected because they would be visible on the nights of observing, have magnitudes greater than eight, and periods shorter than two days because of the length of observing time. One exception on the length of the period was made for Beta Per, because this particular system is a well known and frequently studied system. Observations occurred on the nights of November 30 and December 1 of 2004. Data on each system was taken between two to four hours apart to observe the quadritures of these systems. The data was then converted from text files to spectrographs after it had been reduced and smoothed, using the Excel program. The best spectrographs for each system on both nights of observing are shown in Figures 1.1 through 8.2. Light curves of most of the systems were obtained from the American Association of Variable Star Observers (AAVSO) website.

Information that was essential to calculate the properties of the systems was the apparent magnitudes and the parallax. From the light curves, apparent magnitudes were determined. The Simbad website was also used to receive the parallax of each system. Next, the shapes of the graphs of each system were analyzed to establish what their spectral classes and types were. Temperature was determined by using a table where certain temperatures corresponded to a specific spectra class and type. Distance was determined by using the parallax and formula 1(listed below). This result along with the apparent magnitude was then put into formula 2 to calculate absolute magnitude. Luminosity was determined by using the absolute magnitude of the system, the absolute magnitude of the sun, and the distance to the sun in formula 3. Finally, radius was calculated using the luminosity of the sun and system, the radius of the sun, and the temperature of both the sun and system in formula 4. The results of these calculations can be found in Chart 2.

Formula 1: $D = 1/mas \times 10^3$
·D is the distance
·mas is the parallax value

Formula 2: $m - M = -5 + 5\log(d)$ (M equals absolute magnitude)
·M is the absolute magnitude
·m is the apparent magnitude
·d is the distance

Formula 3: $M(star) - M(sun) = -2.5\log[L(star)/L(sun)]$
·M is the absolute magnitude (the absolute magnitude of the sun is 4.74)
·L is the luminosity (the luminosity of the sun is 3.845×10^{33})

Formula 4: $\frac{L(star)}{L(sun)} = \frac{R(star)^2 \times T(star)^4}{R(sun) \times T(sun)}$
·L is the luminosity
·R is the radius (the radius of the sun is 4.9×10^{21}cm)
·T is the temperature (the temperature of the sun is equal to 1)

Formula 5: delta lambda / lambda (rest) = V / C
·V is the radial velocity of the line
·C is the speed of light

In addition to these calculations, the velocity measurements of the line centers, and the Full Width – Half Maximum or FWHM were also determined. To do this, several elements found in the stars had to be chosen to study. From the spectrographs, ten elements were chosen that were present in all of the systems. Spectral lines that were observed in each system at specific wavelengths (angstroms) were Hydrogen 12, 11, 10, 9, 8, 5, 4, 3, 2, and Calcium II K. The velocity measurement of the line centers is used to find the velocity of the gases of the absorption lines on the graphs. (These absorption lines are the ten elements listed above. The selected lines are only about half of the absorption lines that appear of the graphs.) The first step in finding the line center value is to determine the change in the wavelength of the lines. The resting wavelengths of the ten selected elements give them their identity. However, line wavelengths found on the graphs are different than the resting wavelength because the star system is moving in a red shift (the system is moving away from the observer) or a blue shift (the system is moving toward the observer). To determine this red or blue shift, the recorded wavelength must be subtracted from the resting wavelength. This result, or change in wavelength, is then put into the Doppler formula (see formula 5). Negative values reveal that the system is in a red shift, while positive values reveal the system is in a blue shift. The Full Width – Half Maximum formula is used to calculate the local velocity dispersion of the gas that is forming the absorption lines. This was performed by measuring the velocity width of the spectral lines. The Doppler shift is again invoked to determine this after the following small calculations are made. To begin, each of the selected absorption lines of each graph was enlarged. After this was complete, a line was drawn at the halfway point between the continuum level and center of the flux of line. Two wavelengths were then recorded for each line. These wavelengths are the values of each side of the line at which the halfway point was drawn. The second wavelength was subtracted from the first to again calculate the change in wavelength. This result was then placed into the Doppler formula. The results of the velocity measurements of the line centers and the Full Width – Half Maximum values are listed on the following pages.

Chart 1

Star Name	RA	Dec.	Period (d)	Magnitude
TV CAS	00:19:18.74	59:08:20.55	1.812589	4.28
RZ CAS	02:48:55.51	69:38:03.44	1.1952578	6.267
Beta PER	3:08:41.0	40:57:20.33	2.87	3.1
IQ PER	03:59:44.68	48:09:04.5	1.7435689	7.73
V1061 TAU	04:58:52.76	24:29:44.56	1.385217	8.03
BF AUR	05:05:03.5	41:17:19.11	1.5832227	8.85
VV ORI	05:33:31.45	-01:09:21.86	1.4853762	5.38
R CMA	07:19:28.18	-16:23:42.88	1.1359501	5.7

Chart 2

Star Name	Spectral Class	Temperature	V Magnitude	Distance	B Magnitude	Luminosity	Radius
TV CAS	B9 III	7300K	7.28	254.45 pc	0.25	2.42 x 10^35	6.9 x 10^11cn
RZ CAS	A3 I	8790K	6.27	62.53 pc	2.29	4.61 x 10^34	2.1 x 10^11cn
Beta PER	B8 V	9900K	2.12	28.45 pc	-0.15	3.5 x 10^35	4.5 x 10^11cn
IQ PER	B9 I	9890K	7.73	334.45 pc	0.11	2.73 x 10^35	3.9 x 10^11cn
V1061 TAU	B4 III	12550K	8.03	378.78 pc	0.14	2.65 x 10^35	2.4 x 10^11cn
BF AUR	B5 I	10500K	8.85	50000 pc	-9.64	2.16 x 10^39	3.1 x 10^13cn
VV ORI	B1 III	13540K	5.38	568.18 pc	-3.39	6.8 x 10^36	1.1 x 10^12cn
R CMA	B5 III	12000K	5.7	44.03 pc	2.48	3.07 x 10^34	9.1 x 10^10cn

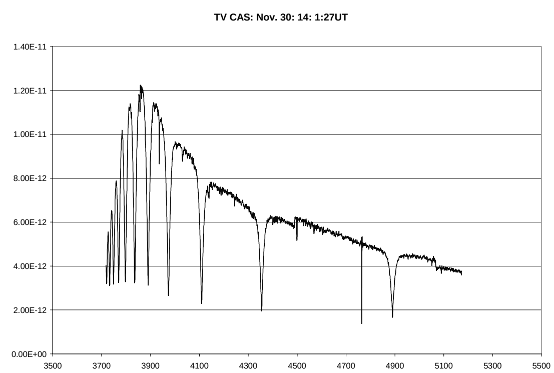

1.1 – TV Cas November 30

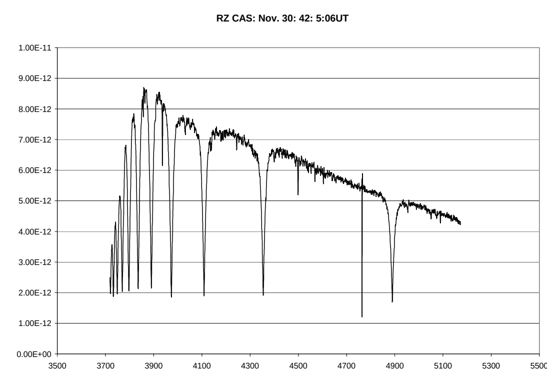

2.1 –RZ Cas November 30

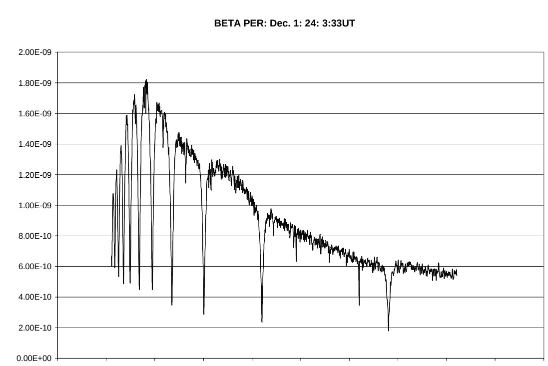

3.2 – Beta Per December 1

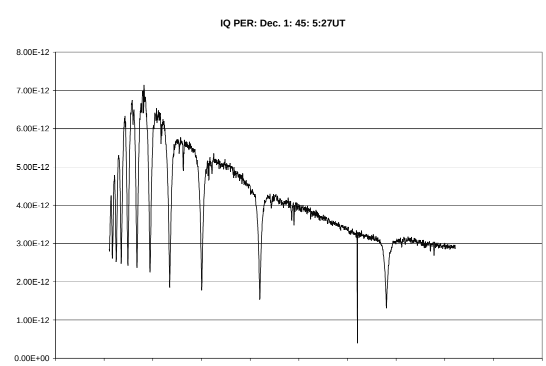

4.2 – IQ Per December 1

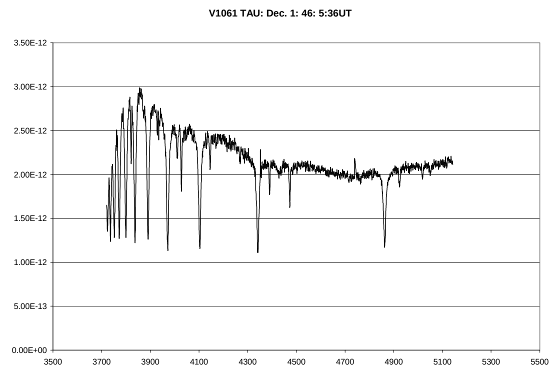

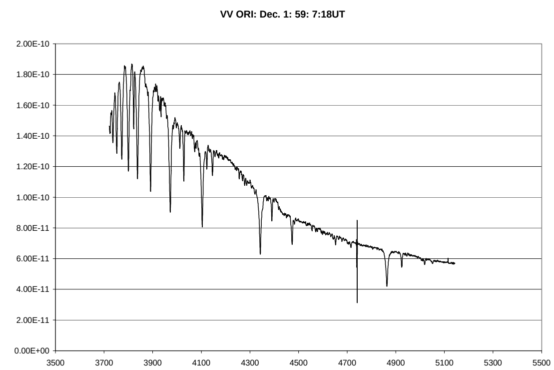

5.2 – V1061 Tau December 1

6.2 - BF Aur December 1

7.2 – VV Ori December 1

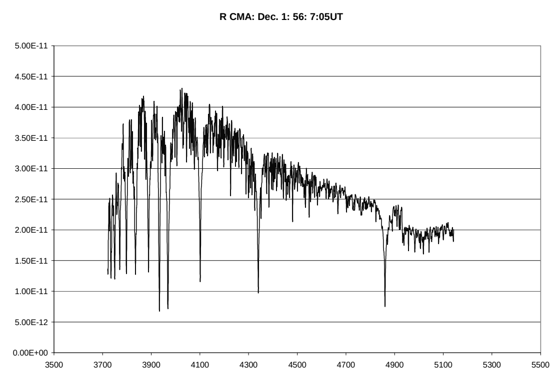

8.2 – R Cma December 1

CONCLUSION

By using spectrographs of eclipsing binary systems, several stellar qualities of these systems were determined. In general, all of the systems' results for each characteristic are appropriate for their spectral type and size. From the spectrographs, the velocity measurements of the line centers and the Full Width – Half Maximums were also computed. These results are helpful in understanding the movement of these eclipsing binary systems. When the system is in blue shift, positive values will be present, while when negative results are present it is indicated that there is a red shift. By analyzing the positive and negative values determined from the FWHM, it appears that the stars within these systems are indeed eclipsing. Had more time been available to observe, a more detailed path of the motion of the stars in the eclipse could have been studied. In addition, systems with longer periods could have been observed as well. However, the findings are sufficient enough for supporting the research questions.

THANKS TO

Dr. Steve Howell and NOAO for the opportunity to observe at Kitt Peak and make this project possible.

Mrs. Beth Thomas for all her support and guidance through out all aspects of the project.

REFERENCES

AAVSO. “AAVSO Light Curve of BETA PER{0301+40} for 2403319 through 2453362.”<*http://www.aavso.org/egibin/superstar2.pl3objectname=Beta+PERlastdays =400&date1=2453319...*> 20 January 05.

AAVSO. “AASVO Light Curve of R CMA{0715-16} for 245319 through 2453362.” <*http://www.aasvo.org/egibin/superstar2.pl?objectname=R+CMA&lastdays=400&date1=2453319...*> 20 January 05.

AAVSO. “AAVSO Light Curve of RZ CAS {0239+69} for 243319 through 2453362.” <*http://www.aasvo.org/egibin/superstar2.pl?obectname=RZ+CAS&lastdays=400&date1=2453319...*> 20 January 05.

AAVSO. “AAVSO Light Curve of TV CAS{0013+58} for 2453319 through 2453362.” <*http://www.aasvo.org/cgibin/superstar2.pl?objectname=TV=CAS&lastdays=400&date1=2453319...*> 20 January 05.

AAVSO. “AASVO Light Curve of VV ORI{0528-01} for 243319 through 2453362.” <*http://www.aasvo.org/egibin/superstars2.pl?objectname=Beta+Per&lastdays=400?date1=2453319...*> 20 January 05.

AAVSO. “Chapter 2-Making Observations : Step by Step Instructions.” Publications. <*http://www.aavso.org/publications/manual/chapter2.shtml*> 14 October 04.

AAVSO. “Chapter 3- About Variable Stars.” Publications. <*http://www.aavso.org/publications/manual/chapter3.shtml*> 14 October 04

AAVSO. “Chapter 4 - Computing the Julian Day & Time.” Publications. <*http://www.aasvo.org/publications/manual/chapter4.shtml*> 14 October 04.

AAVSO. “Types of Variable Stars.” Variable Stars.

<*http://www.aasso.org/vstar/types.shtml*> 18 July 04

AAVSO. “Variable Stars.” Variable Stars. <*http://www.aavso.org/vstar*> 16 October 04.

AURA. “Basic Specifications for the 0.9 Coude Feed Telescope and Spectrograph.” National Optical Astronomy Observatory. 2000.<*http://www.noao.edu/dir /coude/description.html*> 26 September 04.

Croft, Steven and Howell, Steve. Spectroscopy of Variable Stars: Content Background for Stellar Evolution and Variable Star Research. 2004

Emery, Bob “9.7 Astrophysics Continued Page3” Senior Physics and Religion.2004 <*http://webs,mn.catholic.edu.au/physics/emery/hsc.astrophysics.page3.htm*>

22 September 04.

Enchanted Learning. “Astronomy Dictionary.” Zoom Astronomy Glossary. 2004. <*http;//www.enchantedlearning.com/subjects/astronomy/glossary/index-z.shtml*> 14 October 04.

Haselden, Derek. “Astronomical Glossary.” Cyprus Astronomy. <*http:www.cyprusastonomy.com/astronomical%20glossary.html*> 14 October 04.

Isaac Newton Group of Telescopes. “V1061T.” Staralt. <*http;//www.ing.iac.es/ds/staralt/index.php?action=showimage&form…*> 30 November 04.

Isaac Newton Group of Telescopes. “RCMA.” Staralt. <*http://www.ing.iac.es/ds/staralt/index.php?action=showimage&form....*> 30 November 04.

Isaac Newton Group of Telescopes. “VVORI” Staralt. <*http://www.ing.iac.es/ds/staralt/index.php?action=showimage&form...*> 30 November 04

Isaac Newton Group of Telescopes. “BETAPE.” Staralt. <*http://www.ing.iac.es/ds/staralt/index.php?action=showImage&form...*> 30 November 04.

Isaac Newton Group of Telescopes. “BFAUR.” Staralt. <*http://www.ingiac.iac.cs/ds/staralt/index.php?action=showimage&form....*> 30 November 04.

Isaac Newton Group of Telescopes. “IQPER.” Staralt. <*http://www.ing.iac.es/ds/staralt/index.php?action=showImage&form...*> 30 November 04.

Isaac Newton Group of Telescopes. “NCAS.” Staralt. <*http://www.ing.iac.es/ds/staralt/index.php/action=showimage&form...* > 30 November 04.

Isaac Newton Group of Telescopes. “RZCAS.” Staralt. <*http://www.ing.iac.es/ds/staralt/index.php?action=showImage&form...*> 30 November 04.

Kriener, J.M. “AUR.” Up- To–Date Linear Elements of Eclipsing Binaries. <*http://www.as.wsp.krakow.pl/ephem/aur.htm*> 18 October 04.

Kreiner, J.M. “Beta Per.” Atlas of O-C Diagrams of Eclipsing Binary Stars. 2000. <*http://www.as.ap.krakow.pl/o-c/data/getdata.php3?bf%20per*> 18 October 04.

Kreiner, J.M. “BF Aur.” Atlas of O-C Diagrams of Eclipsing Binary Stars. 2000. <*http://www.as.ap.krakow.pl/o-c/data/getdata.php3?bf%20aur.*> 18 October 04.

Kriener, J.M. “Cas.” Up-To-Date linear Elements of eclipsing Binaries. <*http://www.as.wsp.krakow.pl/ephem/cas.htm*> 18 October 04.

Kriener, J.M. “CMA.” Up-To-Date Linear Elements of Eclipsing Binaries. <*http:///www.as.wsp.krakow.pl/ephim/cma.htm* >18 October 04.

Kriener, J.M. “IQ PER.” Atlas of O-C Diagrams of Eclipsing Binary Stars. 2000. <*http://www.as.ap.krakow.pl/o-c/dsts/getdata.php3?iq%20per*> 18 October 04

Kreiner, J.M. “Up-To-Date Linear Elements of Eclipsing Binaries.” <*http://www.as.wsp.krakow.pl/ephem/* > 18 October 04.

Kriener, J.M. “ORI,” Up-To-Date Linear Elements of Eclipsing Binaries. <*http://www.as.usp.krakow.pl/ephem/ori.htm*>18 October 04.

Kriener, J.M. “PER.” Up-To-Date Linear Elements of Eclipsing Binaries. <*http://www.as.wsp.krakow.pl/ephem/per.htm*> 18 October 04.

Kreiner, J.M. “Tables of contents.” Up –To-Date Ephemerides of Eclipsing Binaries. <*http://www.os.ap.krakow.pl/oc/cont.html*> 18 October 04.

Kriemer, J.M. “TALL.” UP –To-Date Linear Elements of Eclipsing Binaries. <*http://www.as.wsp.krakow.pl/ephem/tall.htm*> 18 October 04.

Kriener, J.M. “TV Cas.” Atlas of O-C Diagrams of Eclipsing Binary Stars. 2000. <*http://www.as.ap.krakow.pl/o-c/data/getdata.php3?tv%20eas*> 18 October 04.

Kriener, J.M. “R CMA.” Atlas of O-C Diagrams of Eclipsing Binary Stars. 2000. <*http://www.pl/o-c/data/getdata.php3?r%20cma*> 18 October 04

Kriener, J.M. “RZ Cas.” Atlas of O-C Diagrams of Eclipsing Binary Stars. 2000. *<http://www.as.ap.krakow.pl/o-c/data/getdata.php3?rz%20cas*> 18 October 04.

Kriener, J.M. “V1061 Tau.” Atlas of O-C Diagrams of Eclipsing Binary Stars. 2000. <*http://www.as.ap.krakowpl/o-c/data/getdata.php3?v1061%20tau*> 18 October 04.

Kriener, J.M. “VV ORI.” Atlas of O-C Diagrams of Eclipsing Binary Stars. 2000. <*http://www.as.ap.krakow.pl/o-c/data/getdata.php3?Vv%20ori*> 18 October 04.

Sage, Leslie. and Aschenbrenner, Gail. A Visitor’s Guide to the Kitt Peak Observatories. Cambridge University Press. 2003.

Simbad. “BF AUR.” Simbad Query Result. <*http://simbad,u-strasbg.fr/sim-id.pl?protocol=html&ident=bf+aur&noident=1&radius=10&radius.units* 17 January 05.

Simbad. “BETA PER.” SIMBAD Query Result. <*http://simbad.u-strasbg.fr/sim-id.pl?protocol=html&ident==beta=per&nbiden+=1&radius=10&radius.units…*> 17 January 05.

Simbad. “IQ PER.” SIMBAD Query Result. <*http://simbad.u-strasbg.fr/sim-id.pl?protocol=html&ident=ig+per&nbident+1&radius+10&radius.units…*> 17 January 05.

Simbad. “TV CAS.” SIMBAD Query Result. <*http://simbad.u-strasby.fr/sim-zid.pl?protocol=html&tdent=tv+casnbident=1&radius=10&radius.unit…*> 17 January 05.

Simbad.”R CMA.” SIMBAD Query Result. <*http://simbad.u-strasbg.fr/sim-idpl?protocol=html&ident=vv+ori&nbident=1&raduis=10&raduis.units.…*> 17 January 05.

Simbad. “RZ CAS.” SIMBAD Query Result. <*http://simbad.u-strasbg.fr/sim-id.pl?protocol=html&ident=rz+cas&notdent=1&radius=10&radius.unit…*>
17 January 05.

Simbad.”V1061 TAU.” SIMBAD Query Result.*http://simbad.u-strasbg.fr/sim-id.pl?protocol=html&ident+v1061+tau&Nbident=1&radius=10&radius.units..*
17 January 05.

Sinbad. “VV ORI.” SIMBAD query Result. <*http://simbad.u-strasbg.fr/sim-id.pl&protocol=html=vv+ori&ident=1&radius=10&radius.units…*>
17 January 05.

Simonsen, Mike. “Observing Variable Stars.” Observing Variable Stars. <*http://home.earthlink.net/~joevp/docs/observing.ms.htm*> 21 September 04.

Steve Howell and Steven Croft. Telephone interview. 28 October 04.

Steve Howell. Telephone interview. 15 November 04.

Ware, Don. “Binary Stars.” Peoria Astronomical Society. 2004. <*http://www.astronomical.org/astbook/binary.html*> 22 September 04.

A Study of Host Stars in Comparison with Stars without Planets, Using Spectrographs

Michelle Smith
Great Falls High School, Great Falls, MT
Teacher: Beth Thomas, TLRBSE 2004

ABSTRACT

In this project the spectra of a host star, a star with an orbiting planet, was compared to the spectra of a star without a planet of the same spectral type and luminosity class. The purpose of collecting this data was to narrow scientists search for extra-solar systems. I hypothesized that if the absorption lines in the stars without planets, expressed in a spectrograph, differed from the lines in a host star, creating a trend, this trait could then be used to further explore the universe and to identify other extrasolar systems. Five pairs of stars were studied, each pair consisting of a star without a planet and a host star, each of the same spectral type and luminosity class. A wide array of the element absorption lines can be view through spectrographs; each element is emitted at a specific wavelength from the stars themselves. The primary data-collecting tool was the Coudè Feed telescope, located at the Kitt Peak Observatory in Tucson, Arizona. The data came in a text format that was later converted into spectrographs using the excel spreadsheet program. With the information from the spectrographs stellar surface temperature, spectral type, luminosity class, and radius were calculated. The stars were compared using calculations, techniques and the spectrographs. The data partially supported my hypothesis; it is possible to distinguish between two stars by their spectrographs. In three of the five pairs studied, the absorption lines of the host stars had a higher flux than the absorption lines of the standard star. In the remaining pairs, absorption lines of the standard star emitted a higher flux than the absorption lines in the host star.

INTRODUCTION

I hypothesized that if the absorption lines in the standard star differed from the lines in a host star, creating a trend, this trait could then be used to further explore the universe and to identify other extrasolar systems. Current research suggests that extrasolar systems are rare and difficult to identify, so I hope, through my research, to reduce the difficulty of this search. If a spectral trait is found consistently then one could easily take the spectra of a possible extrasolar system and compare it to several standard star spectrographs (of the same spectral type and luminosity class). Further comparisons could allow scientists to determine whether or not a star is worthy of extensive study.

The Coudè Feed Telescope was used because of the high precision spectra it produces. The Coudè Feed telescope is one of many National Optical Observatories at Kitt Peak. The data collected of the stars observed was recorded to a database for later computer analysis. Dr. Steve Howell smoothed and reduced the data before sending it to me in a text format. This smoothing and reduction was to dispose of pollution to the spectrograph done by the atmosphere.

An observing schedule was created and organized by Right Ascension. Each night of observing the telescope was calibrated to meet my project's requirements. Camera 5 was used for moderate/high spectral resolution, and the Flat (Quartz) Lamp was utilized because it is common lamp for calibration spectroscope. The blue region was the observe area of the spectrum; this area stretches from about 3700 to 5300 angstroms. An example of the overlapped spectrographs bellow:

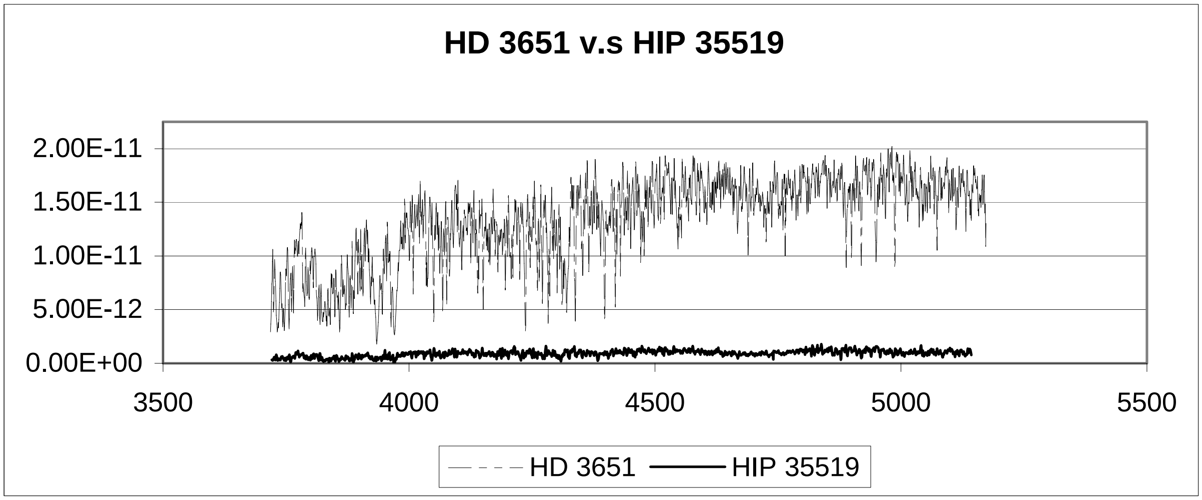

This graph shows stars HD 3651 and HIP 35519, a host and standard star, respectively. When looking at the spectrograph you see that the two graphs have similar absorption lines but the absorption line fluxes are different. This happened in all pairs of stars.

ANALYSIS

Once the datawas converted into graphs ,using the Excel spreadsheet program, I used the following techniques to make some critical determinations:

- ***Surface Temperature* - To determine the stellar surface temperature the stars the spectral type and class is compared to find the stars average temperature. The temperature chart available in the literature:" Spectroscopy Variable Stars Content Background for Stellar Evolution and Variable Star Research." Howell, Steve and Croft, Steven. , was used.**
- ***Apparent Magnitude* - The apparent magnitude was found through the Simbad Query Form. It was shown for each star as they were researched.**
- °*Distanc*e - **The Hippoarcos/TYCHO archives were used to find the parallax. The to calculate the actual distance, following equation use to calculate distance: d=1/parallex in arcsec.**

After figuring the distance, the apparent magnitude was inserted into the equation bellow, long with the distance to calculate the absolute magnitude:

m (apparent Magnitude)-M (absolute magnitude)=-5+5log d

Star Comparisons

Chosen Stars	Spectral Type	Luminosity Class	Temperature	Apparent Magnitude	Distance	Luminosity	Absolute Magnitude	Stars Radius
HD 3651	K0	V	5250	5.8	11.107 pc	-1.8051	5.579261	1.1469*10^11
HIP 35519	K0	V	5250	8.6	50.916 pc	0.4838	4.066	5.9381*10^10
HD 10997	A3	V	8585	8.1	406.50 pc	21.69	0.0546	1.4896*10^11
HD 10638	A3	V	8585	6.7	71.684 pc	32.486	2.423	1.8197*10^11
HD 38529	G4	IV	5315	5.93	42.42 pc	23.168	2.7921	4.0086*10^11
HD 37124	G4	IV	5315	7.68	33.24pc	2.833	5.0716	1.4020*10^11
HD 4413	F8	V	6200	10.86	27.744 pc	1.9448	4.01	8.5367*10^10
HD 50554	F8	V	6200	6.86	31.02 pc	5.0607	4.4017	1.3770*10^11
Upsilon Andromedae	F8	V	6200	4.09	13.46 pc	12.695	3.4431	2.1810*10^11
HD 4413	F8	V	6200	10.86	27.744 pc	1.9448	4.01	8.5367*10^10

°***Luminosity*** – The following equation was utilized**:**

M (absolute magnitude. of star)- M (sun)=-2.5log (L (star)/(L (sun))

Example: 7.89 * 10^33 .The 10^33 is understood so the luminosity would be **7.89**

°*Radius* - R/**R** $_{sun}$ **= (T** $_{sun}$ **/T)^2 SQRT (L/L** $_{sun)}$**-** This equation calculates the radius**.** An example problem is as follows**: R** $_{rigel}$ **/ R** $_{sun}$ **= (1/3)^2 SQRT (64,000) =27.5**

Spectra Analysis**:** A list of several spectral lines common to host star and standard star pair was chosen, using these selected spectral lines. Using this list I constructed graphs that compared the selected absorption line fluxes. The elements and molecular band absorption lines are as follows with the corresponding resting wavelength in Angstroms: H Beta 4861, H Gamma 4340, H Delta 4101, H Epsilon 3970, He I 3965, Ca I 4226, Ca II K 3933.7, Ca II H 3968.5, G molecular band 4314, C2 Swan Band 5165, TiO 4954, CN 4217, CIII 4056 and C2/SiC 4640.

DISCUSSION

Stars HD 3615 and HIP 35519 are in luminosity class five, and are spectral type K0 stars. Each star showed strong Calcium Hydrogen and Potassium lines. The main difference in the graphs was the flux. While HD 3651 flux range was between 1.79 E-12 mμ and 2.02 E11 mμ, while HIP 35519 flux ranged from 1.59 E-13 mμ to 1.69 E-12 mμ. This difference happened in all of the star pair graphs.

On the chart title “Star Comparisons” you can see the two stars compared. Notice their luminosity and absolute magnitude are similar but their sizes vary the most.

HD 10997 and HD 10638 are the A3 class five stars. Their spectrograph fluxes where amazingly different, however they both showed strong absorption lines in the Calcium H and K lines and an amazing curve common to that star class. This pair was one of two pairs where the star with out planets had a larger flux then the host stars flux. HD 10997 highest point in recorded to the graph lies at 1.29E-12 mμ and it’s lowest at

1.13E-13 mμ. HD 10638's highest recorded flux was at 1.58E-11 mμ and it's lowest at 1.75E-12 mμ.

HD 38529 and HD 37124 are the G4 luminosity class four stars studied. In this pair the spectra curves were not as similar are the rest of the observe stars. While HD 38529 showed the expected curve HD 37124 looked as if it started to flat line toward the end. HD 38529 has the large flux range of the two and is also the host star. The absorption line fluxes more define then those of star HD 37124. Also star HD 38529 is almost three times the size of star HD 37124.

Stars HD 50554 and HD 4413 are class five, spectral type F8 stars. When the two stars were compared HD 4413's absorption line fluxes were larger then the fluxes of star HD 50554. This pair was the only other stars I studied that the star without a planet had larger flux lines them the host star. However the stars flux lines nearly overlap each other. Star HD 4413's lowest flux line lies at 7.47E-12 mμ and its highest at 7.63E-11 mμ, while HD 4413's highest flux reached 1.37E-11 mμ and its lowest hit 1.77E-12 mμ. The areas where the graphs overlapped were the Calcium H and K lines

Upsilon Andromedae and HD 4413 was the only stars compared that visually overlapped each other. Upsilon Andromedea's lowest flux was at 1.67E-11 mμ and its highest flux ranged up to 1.37E-10 mμ and HD 4413's highest flux was at 1.37E-11 mμ and its lowest hit 1.77E-12 mμ. Upsilon Andromedae flux was larger then HD 4413's flux but not so much that they didn't overlap.

Using these techniques the values where calculated to thoroughly compare the host stars with their comparison stars. The differences in the fluxes of the stars were expressed by subtracting the host stars flux, for the particular absorption line, from the flux number of the standard stars. In two sets of stars, negative numbers were the result and in three positive numbers dominated. When viewing the graph you may notice that each pair of stars information is extremely similar so the real analysis lies in the spectrographs themselves.

Spectra of the selected stars were collected for two nights and each night the Dewar was filled to keep the CCD Detector cool, which is vital to obtain high-quality spectra. Then, around five o'clock P.M (winter) we went atop the roof to open the tower, the cover for the light tube and the shed that covered the largest lens. The light hits the largest lens and is reflected to the tower to a second mirror. The light is then reflected a second time to the light tube (on the other side of the shed) and down to the actual spectroscope. While we opened and set up the telescope, all the equipment was off. We then entered the control room (all other lights were off) to take the spectra of a standard bright star to zero in the telescope. The chosen star was on the Right Ascension directly above us, this told the telescope where it was in the universe. Then, I would choose my first star to observe, and my partner (also in control of the log book) would type in the coordinates. In the logbook she recorded the following: Disk Pic. number (its number in the database), the names of the observed object, its magnitude, the integration time and the start of the time in universal increments. I would start the integration time— the stars light exposure time to the light detectors—and check the spectrographs as they were received to verify clarity. Once the integration time was up, Kimm recorded the time in the logbook and we repeated the process over again. Around 7 A.M, we would close the shed over the telescope, fill the Dewar, and go to sleep. By the second night we had the process down to an art and collected 94 spectra!

There were many variables in the experiment, including the atmosphere. When observing we could not effectively observe stars when the Airmass was greater then two, —a measurement of the atmospheric thickness in that area of the sky. During observation, the farther toward the horizon the desired objects sat, the thicker the air mass became. The light detector is a very delicate tool; exposure to too much light can damage it. While taking spectra you can over expose or under expose the spectroscope —not allowing the correct amount of time for the magnitude of the star can distort the data for the spectrograph. Noise was also a big variable; which is caused when the spectroscope detects stray light. Noise is an uncontrollable event, along with time constraints and cloudiness.

Three to four comparison stars would be the desirable amount for each host star in order to have more accuracy. I was very grateful for the amount of time I was given to explore this, however, to fully support my hypothesis, spectra would need to be taken several times in a year of different host stars and multiple stars, of the same luminosity class and spectral type, without planets

SUMMARY AND ACKNOWLEDGEMENTS

The absorption lines of the star without the planet were shallower in the groups of HD 50554 and HD4413, and HD 10997 vs. HD10638 of the stars I analyzed. In the pairs Upsilon Andromedae and HD 4413, HD 3615 and HIP 35519 and HD 38529 and HD 37124 the host stars absorption lines were shallower than the standard star's. With this information my hypothesis is partially proven in that then look at the spectra of two and differentiate between the two. I would like to thank Mrs. Beth Thomas and Dr. Steve Howell; they were my mentors and major supporters throughout this project. Thank you NOAO funding the program that allowed me to work on Kitt Peak for two full nights! Also, I would like to thank my parents for without them I wouldn't have gone very far with this project. Finally I'd like to thank all of the staff and fellow observers I met on while in Tucson. My life has been forever changed for the better because of your words of advice and encouragement. It's always a good feeling to know there are dozens of well-educated people out in the world who share in my same interests. Future students can use this research as a guide, or perhaps a springboard to start future project on spectra. Either way I hope that people remember that indeed our futures do lie ultimately in the stars.

BIBLIOGRAPHY

Chartrand, Mark R. (2001) Field to the Night Sky "The Universe" P 13- 96"

Cowen, Ron. "More Planets" October 16, 2004. 1997 *http://web1.infotrac.galegroup.com/itw/infomark/184/287/52853078w1/purl=rc1_EAIM_0_A19482749&dyn=55!xm_10_0_A19482749?sw_aep=mtlib_a_greatfal*

Howell, Steve and Croft, Steven. " Spectroscopy Variable Stars Content Background for Stellar Evolution and Variable Star Research" March 2003.

Lehmuskalio, Jouko / Rec Button Oy And Paal Brekkee. Soho "Exploring the Sun" 2003, October 20, 2004

Marcy, Groffery W. and Butler, R. Paul "Giant Planets Orbiting Faraway Stars" October 16 2004
http://astron,berkley.edu/~gmarcy/sciam.html

The Isaac Newton Group of Telescopes. "Staralt v2.3." 2005.November 30, 2004.
http://www.ing.iac.es/ds/staralt/index.php

Schneider, Jean "Notes for HD 3651" 16 Jan, 03 26, Jan 04
http://www.obpsm.fr/encyl/HD3651.html

Schneider, Jean "Notes for HD 6434" 16 Jan, 03 26, Jan 04
http://www.obpsm.fr/encyl/HD6434.html

Schneider, Jean "Notes for HD 12661" 16 Jan, 03 26, Jan 04
http://www.obpsm.fr/encyl/HD12661.html

Schneider, Jean "Notes for HD 37124" 16 Jan, 03 26, Jan 04
http://www.obpsm.fr/encyl/HD37124.html

Schneider, Jean "Notes for HD 38529" 16 Jan, 03 26, Jan 04
http://www.obpsm.fr/encyl/HD38529.html

Schneider, Jean "Notes for HD 46375" 16 Jan, 03 26, Jan 04
http://www.obpsm.fr/encyl/HD46375.html

Schneider, Jean "Notes for HD 50554" 16 Jan, 03 26, Jan 04
http://www.obpsm.fr/encyl/HD50554.html

Schneider, Jean "Notes for HD 73526" 16 Jan, 03 26, Jan 04
http://www.obpsm.fr/encyl/HD73526.html

Schneider, Jean "Notes for HD 8574" 16 Jan, 03 26, Jan 04
http://www.obpsm.fr/encyl/HD8574.html

Seeds, Micheal A., "Foundations of Astronomy 2003". October 14, 2004

Winters, Jeffrey "Planets, Planets Everywhere" 1996 October 16, 2004
<http://web1.infotrac.galegroup.com/itw/infomark/184/287/52853078w1/purl=rc1_EAIM_0_A18107918&dyn=55!xm_1_0_A19482749?sw_aep=mtlib_a_greatfal